DEVELOPMENT OF NUCLEIC ACID COATED NANOPARTICLE BASED LATERAL FLOW ASSAY FOR *SALMONELLA* DETECTION

THESIS SUBMITTED TO
THE GRADUATE SCHOOL OF NATURAL AND APPLIED SCIENCES OF
MIDDLE EAST TECHNICAL UNIVERSITY

BY

MÜSLÜM KAAN ARICI

IN PARTIAL FULFILLMENT OF THE REQUIREMENTS
FOR
THE DEGREE OF MASTER OF SCIENCE
IN
BIOTECHNOLOGY

SEPTEMBER 2017

Approval of the thesis:

DEVELOPMENT OF NUCLEIC ACID COATED NANOPARTICLE BASED LATERAL FLOW ASSAY FOR *SALMONELLA* DETECTION

submitted by **MÜSLÜM KAAN ARICI** in partial fulfillment of the requirements for the degree of **Master of Science in Biotechnology Department, Middle East Technical University** by,

Prof. Dr. M. Gülbin Dural Ünver
Dean, Graduate School of **Natural and Applied Sciences** _____

Assoc. Prof. Dr. Çağdaş Devrim Son
Head of **Biotechnology Department, METU** _____

Prof. Dr. Meral Yücel
Supervisor, **Biological Science, METU** _____

Prof. Dr. Hüseyin Avni Öktem
Co-Supervisor, **Biological Science, METU** _____

Examining Committee Members:

Assoc.Prof.Dr. Ayşe Elif Erson Bensan,
Department of Biological Science, METU _____

Prof. Dr. Meral Yücel
Department of Biological Science, METU _____

Prof. Dr. Hüseyin Avni Öktem
Department of Biological Science, METU _____

Asst. Prof. Dr. Oya Ercan Akça
Department of Molecular Biology and Genetics, Harran University _____

Asst. Prof. Dr. Mahmut Deniz Yılmaz
Department of Bioengineering, Konya Food and Agriculture University _____

Date: 08.09.2017

I hereby declare that all information in this document has been obtained and presented in accordance with academic rules and ethical conduct. I also declare that, as required by these rules and conduct, I have fully cited and referenced all material and results that are not original to this work.

Name, Last name	**:**	**Müslüm Kaan ARICI**
Signature	**:**	

ABSTRACT

DEVELOPMENT OF NUCLEIC ACID COATED NANOPARTICLE BASED LATERAL FLOW ASSAY FOR *SALMONELLA* DETECTION

Arıcı, Müslüm Kaan

M.S., Department of Biotechnology

Supervisor : Prof. Dr. Meral Yücel

Co-Supervisor : Prof. Dr. Hüseyin Avni Öktem

September 2017, 83 Pages

Advances in nanomaterials have promoted the development of biosensor technologies. User friendly, fast, economic, reliable biosensors can be incorporated into diagnostic methods. Without complex laboratory equipment and qualified person, Point of Care (PoC) tests with biosensors can be carried out. Among a variety of biosensors, nucleic acid based biosensors are promising to have high specificity and sensitivity. Thus, in this study, nucleic acids are employed on modifications of nanomaterials during construction of lateral flow assay (LFA) platform.

Foodborne diseases continue to be a major health issue. A major reason of foodborne disease is *Salmonella* contamination. Contaminated foods give rise to serious illnesses, possibly hospitalization and death if untreated. Consequently; safe, rapid and economic detection methods of *Salmonella* is likely to improve public health.

The aim of this study is detection of *Salmonella* with LFA including mesoporous silica nanoparticles (MSP-SiNPs). In this study, MSP-SiNPs, entrapping 3,3',5,5'-Tetramethylbenzidine (TMB), were functionalized with oligonucleotide

probes, which were complementary sequences to *InvA* gene of *Salmonella*. Complementary target sequence took oligonucleotides away from SiNPs and made TMB released so that HRP-H_2O_2 can oxidize TMB. Optimization experiments were carried out to get proper colorimetric reaction on LFA,.

In our study, optimized LFA platform could manage high specificity. 284 bp amplicon of *InvA* gene and 292 bp amplicon of *Ycdt* gene were significantly discriminated by complementary probes. Probes could considerably differentiate targets and 3 mismatches on complementary sequences. Sensitivity of SiNPs based LFA was also checked with synthetic targets and PCR. Limit of Detection (LoD) for synthetic complementary target reached up to l5 nM. LoD for PCR was found at 15 cycle.

SiNPs based LFA system, advanced in this study, achieved to specifically and sensitively detect *Salmonella* through target amplicon. The device is promising, hopeful and up-coming for undeveloped countries to do a field study. SiNPs based LFA is a cheap, rapid, reliable and user-friendly detection system.

Keywords: Lateral Flow Assay, Silica Nanoparticle, *Salmonella*, Biosensors

ÖZ

SALMONELLA TANISI İÇİN NÜKLEİK ASİT KAPLANMIŞ SİLİKA NANOPARÇACIK TABANL YATAY AKIŞ TESTİNİN GELİŞTİRLMESİ

Arıcı, Müslüm Kaan

Yüksek Lisans, Biyoteknoloji Bölümü

Tez yöneticisi : Prof. Dr. Meral Yücel

Yardımcı Tez Yöneticisi : Prof. Dr. Hüseyin Avni Öktem

Eylül 2017, 83 Sayfa

Nanomalzemelerdeki ilerlemeler biyosensör teknolojilerinde gelişmelere katkıda bulunmuştur. Kolay kullanılır, hızlı, ekonomik, güvenilir biyosensörler teşhis yöntemleriyle birleştirilebilir. İleri laboratuvar ekipmanları ve yetişmiş eleman olmaksızın biyosensörlerle hasta başında testler yapılabilmektedir. Nükleik asit tabanlı biosensörler yüksek özgüllük ve seçicilik için umut vaat edicidir. Bu yüzden, bu çalışmada olduğu gibi nükleik asitlerle nanomalzemeler üzerinde değişiklik yapılır ve yatay akış test (YAT) platformlarına yerleştirilir.

Gıda kaynaklı hastalıklar toplum sağlığı için tehdit olmaya devam etmektedir. Gıda kaynaklı hastalıkların en büyük sebebi *Salmonella* bulaşmasıdır. Kontamine olmuş besinler klinik bakıma ve tedavi edilmezse ölüme sebep olan ciddi hastalıklara yol acar. Sonuçta güvenilir, hızlı ve ekonomik *Salmonella* tanılama yöntemleri halk sağlığı sistemlerinin işleyişini hızlandıracak ve iyileştirecektir.

Bu çalışmanın amacı mezoporlu yapıda silika nanoparçacık (MZG-SiNP) içeren YAT ile *Salmonella* tanılamaktır. Bu çalışmada, 3,3’,5,5’-Tetramethylbenzidine (TMB) yakalamış MZG-SiNP, *Salmonella InvA* genine tümler sekanslardan oluşan oligonükleotide problarla fonksiyonel hale getirildi. Tümleyici hedef

sekans oligonükleotitleri SiNP yüzeyinden probları uzaklaştırdı ve TMB'nn salınımı sağladı. Böylece, HRP-H2O2 TMB'yi oksitleyebildi. YAT üzerinde uygun bir kolorimetrik reaksiyon elde etmek için optimizasyon deneyleri yapıldı.

Optimize edilmiş YAT'i yüksek seçiciliği başarabilmiştir. Tümleyici problar *InvA* geninin 284bp'lik amplikonu ve *YcdT* geninin 292bp'lik amplikonu ayırt edebilmiştir. Ayrıca, problar hedef ve sekanslardaki 3 yanlış eşleşmeyi de ayırt edebilmişlerdir. SiNP tabanlı YAT'ların duyarlılığı sentetik hedefler ve PZR ile kontrol edilmiştir. Sentetik hedef için tespit sınırı 15 nM'a ulaşmıştır. PZR için tespit sınırı 15 tekrar bulunmuştur.

Bu çalışmada geliştirilen SiNP tabanlı YAT sistemi seçici ve duyarlı olarak *Salmonella*'yı hedef amplikon ile teşhis etmeyi başardı. Gelişmemiş ülkelerin saha çalışmaları için bu araç gelecek vaat eden ve umut veren bir araçtır. SiNP tabanlı YAT ucuz hızlı güvenilir ve kullanımı kolay bir tanılama sistemidir.

Anahtar Kelimeler: Yatay Akış Testi, Silika Nanoparçacık, *Salmonella*, Biyosensör

To My Family…

ACKNOWLEDGEMENTS

I present my greatest gratitude to my supervisor Prof. Dr. Meral Yücel and my Co-supervisor Prof. Dr. Hüseyin Avni Öktem for their precious guidance, endless support, encouragement and inspiringly mentoring. I always feel pride of being a member of YÜCEL and ÖKTEM laboratory group.

I would like to thank to examing committee members; Assoc. Prof. Dr. Ayşe Elif Erson Bensan, and Asst. Prof. Dr. Mahmut Deniz YILMAZ for their contributions to my thesis.

I would like to express my sincere appreciation to Asst. Prof. Dr. Oya Ercan Akça and Asst. Prof. Dr. Çağla Sönmez for sharing many treasured knowledges with me and valuable advice during my thesis. Without their helps and shares, this study would not have been carried out.

I also wish to give my special thanks to Onur Bulut for his endless patience, moral support, participation, and comments about my studies.

I am thankful to past and present my laboratory mates; Dilan Akın, Işkın Köse, Evrim Elçin, Onur Bulut, Ayşegül Öktem, Tuğçe Ceren Tuğrul, Evrim Aksu one by one for their priceless friendship, moral support and valuable comments.

I am truly grateful to my wife, Ezgi Tekin Arıcı, and my parents, Kamil Arıcı and Satı Arıcı, my sisters İlknur Erarslan and Evrim Arıcı for their invaluable moral support and endless patience.

This study was supported by METU, BAP-07-2014-007-616 and Nanobiz R&D limited. I am thankful to METU central laboratory for their technical supports.

TABLE OF CONTENTS

LIST OF TABLES

TABLES

LIST OF FIGURES

FIGURES

LIST OF ABBREVIATIONS

APS	**:**	3-aminopropyl trimethoxysilane
CdS	**:**	Cadmium Quantum Dots
DNA	**:**	Deoxyribonucleic acid
AuNPs	**:**	Gold Nanoparticles
HF	**:**	Hi-Flow
HRP	**:**	Horseradish Peroxidase
LFAs	**:**	Lateral Flow Assays
LBA	**:**	Luria Bertani Agar
LBB	**:**	Luria Bertani Broth
LoD	**:**	Limit of Detection
MSP	**:**	Mesoporous
MSP-SiNPS	**:**	Mesoporous Silica Nanoparticles
PCR	**:**	Polymerase Chain Reaction
PBS	**:**	Phosphate Buffer Saline
PoC	**:**	Point of Care
QDs	**:**	Quantum Dots
RNA	**:**	Ribonucleic acid
SiNPs	**:**	Silica Nanoparticles
Ss	**:**	Single stranded
TMB	**:**	3,3′,5,5′-Tetramethylbenzidine
TSA	**:**	Tryprtic Soy Agar
TSB	**:**	Tryprtic Soy Broth

CHAPTER 1

INTRODUCTION

1.1. Biosensors

Biosensing has been proceeded both at technology of biosensor and applications of biosensors due to innovative entries with electrochemistry, nanotechnology and bioelectronics since the first biosensor to measure glucose was reported by Clark in 1953, (Vigneshvar, 2016). The development of biosensing technologies has been succeeded in biomedical and environmental application for the last decade. Especially, in undeveloped countries, the presence of biosensors for common diseases helps to save lives (Claudie Parolo and Arben Merkoçi, 2013).

Biosensors are biological sensing devices which can provide specific analytical information about analyte or target molecule. Biosensors are composed of biochemical recognition system and physico-chemical transducer (Thevenot, 2001). Biochemical recognition system can include biological molecules such as enzymes, antibodies, receptors, nucleic acids or biomimetic molecules, aptamers, peptide nucleic acids, ribozymes, ionophores. (Scheller, 2001). Thanks to the high specificity of biochemical recognition systems, biosensors gained a high selectivity. The recognizer interacts with target molecule and the recognition system is in contact with physico-chemical transducers which transform the output signal of recognition system to electrical domain so that quantifiable electric signal or other measurable signals can be recorded. As a result, biosensors can achieve the quantification and detection of target molecule (Thevenot, 2001).

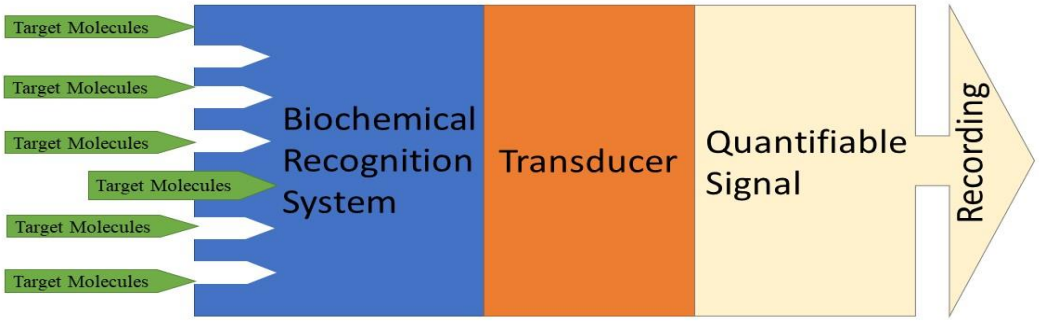

Figure 1.1: Overall scheme of biosensors

Biosensors have a wide range of applications such as, diagnosis, drug discovery and delivery, biomedicine, food safety and process control, environmental monitoring (Vigneshvar, 2016). They are used in the identification of various substrate, metabolite and contaminants (Linda Dekker, Karen M Polizzi, 2017);(Sun-Mi Lee et al., 2016)

Technological advances and utilization of new smart materials enable biosensors to work with high sensitivity and specificity. Especially, the usage of nanomaterials in biosensors have created fabulous nanobiosensors. Real-time analysis, high throughput screening, label-free detection and low limit of detection can be sufficiently provided with nanobiosensors (Sun-Mi Lee et al., 2016).Especially, colorimetric biosensors serve as an easy-to-handle, cost effective diagnosis.

Biosensors are also employed in food and drink industries which govern biosensors for production units to check raw materials, product quality and the manufacturing process (Mello, 2002). Concerning environmental usage, biosensors are used various fields from the detection of pesticides to bioremediation of toxic materials (Verma, 2017) (Hassani, 2017).

To get adequate biosensors, biosensors should verify the definition of diagnostics method. World Health Organization (WHO) defined diagnostics as ASSURED: Affordable, Sensitive, Specific, User-Friendly, Rapid, Equipment-free ad Deliverable to end-users (Claudie Parolo and Arben Merkoçi, 2013). These features depend on a selection of biosensors' components and environmental conditions such as pH, ionic strength, temperature etc. Thus, to design a successful biosensor, types of all components and environmental conditions must be taken in consideration by checking classifications of components and their properties.

1.2. Nanomaterials in Biosensors

The cost of biosensors, inadequate laboratories and the lack of trained people are widespread problem in undeveloped countries. Nanomaterials brings about advantageous solution to these problems via participating the design process of novel biosensing systems (Claudie Parolo and Arben Merkoçi, 2013). Additionally, nanomaterials improve performance of biosensors by increasing specificity and lowering limit of detection with their unique properties and surface characteristics. Additionally, nanomaterials improve performance of biosensors by increasing sensitivity and lowering limit of detection since the surface of nanomaterials allows to enhance the quantity of biorecognition units (Michael Holzinger, Alen Le Goff and Serge Cosnier, 2014).

Nanomaterials have the high specific surface area which enhancing the quantity of recognition units. However, recognition units can not directly interact with the surface of nanomaterials. The surface must be biofunctionalized via covalent binding or non-covalent approaches such as electrostatic interaction, packing in polymers, π-π stacking etc. It is critical to maintain their appropriate biofunctionalization in physiological media and preserve their biological activity during application (R. M. Fartila, S. G. Mitchell, P. D. Pino, V. Grazu and J. M. Fuente, 2014). The presence of other proteins, nucleic acids or chemicals apart from analyte generally disrupt biofunctionalization. Particularly, non-covalent functionalization does not sustain stability and reproducibility. On the other hand, covalent functionalization enhances stability and reproducibility. Amide coupling

reactions, cross linking or click chemistry can form covalent bound. A weakness of covalent links is uncontrolled anchoring of recognizing molecule on nanomaterials, which damages the sensitivity of biosensors (Michael Holzinger et al., 2014).

Biofunctionalization takes place with immobilization of biochemical molecules on the surface of nanomaterials. Biochemical molecules are immobilized to surfaces via supramolecular. Usefully, biosensors with supramolecular can be reutilized because supramolecular makes biosensors reversible by regenerating transducer elements. Nanomaterials can be equipped with proper functionalization methods by coating or capping. Functionalization methods depend on nanomaterial types. Thus, properties of nanomaterials should be well known. Various nanomaterials have been used in biosensing technologies (Michael Holzinger et al., 2014). Gold nanoparticles, quantum dots, magnetic nanoparticles, carbon nanostructures etc. are commonly used but silica nanoparticles, other dyed beads, liposomes are also academically studied.

From ancient times to present, gold has been used for various application in medicine. Nowadays, various types of gold nanoparticles (AuNPs) such as nanospheres, nanorods, nanocubes of 2 to150 nm are utilized in both market and facilities. AuNPs have the ability of strong light absorption and the ability of light scattering. For both visible and infrared range, adjusting their size and shape gets AuNPs applicable in biosensing technologies. The chemical properties of AuNPs support easy and controllable attachment of recognizer (Nur Mustafaoglu, Tanyel Kiziltepe, Basar Bilgicer, 2017). The size, shape of AuNPs and dielectric constant coming from its environment act on configurability. These environmental factors generate bioanalytics because recognition drives to a change of color which can be observed by naked eyes (Michael Holzinger et al., 2014).

Quantum dots are luminescent semiconducting nanocrystals made up of various materials such as cadmium, graphene, carbon etc. Typical size of QDs is in the diameter range of 1-10 nm and contains 100 to 10,000 atoms. QDs have been efficiently combined with biochemical recognizers, adjustable photoluminescence

with long-photostability, which offers advantage in biological applications such as bioimaging, biotargetting and biolabeling (Dan Mo and Liang Hu, 2017). Energy transfer between QD and accepter molecules (quencher) creates the recordable signals. By setting the distance between quencher and accepter molecules get QDs to be tunable and predictable. (Michael Holzinger et al., 2014).

1.3. Mesoporous Silica Nanoparticles

Various silica nanoparticles (SiNPs) are accepted as good candidates in biosensing technologies. SiNPs have been in place of various fields of biomedical applications: biosensors, cell imaging, cell and biomolecular separation, drug delivery, gene therapy etc. (Tatiana Andreani, Amelia M. Silva, Eliana B. Souto, 2015). SiNPs offer many advantages in biosensing sciences, listed below.

- High hydrophilicity
- Appropriate for preparation, separation and synthesis
- Biocompatible, non-toxic
- Transparency to allow excitation light and emission light pass through
- Convenient for modification with various functional group
- Controllable particle size (W. Zhang, X. X. Hu, X. B. Zhang, 2016).

IUPAC classify porous materials into microporous (<2 nm), mesoporous (2-50 nm) and macroporous (>50 nm). Even though microporous materials have high surface area, their porosity is insufficient to accommodate large molecules. Thus, their performance is restricted due to limited diffusion coming from smaller pore sizes. Thus, industrial and academic researchers have focused on expanding pore size from microporous to mesoporous (D. Rath, S. Rana and K. M. Parida, 2014).

After achieving nano-sized mesoporous silicas, Mesoporous (MSP) SiNPs gained popularity because of adjustable morphologies, dimensions, pore sizes and pore structures. During synthesis of MSP-SiNPs, the pH of reaction, surfactants or

copolymers, concentrations of silica and sources of silica define properties of MSP-SiNPs (S. H. Wu, C. Y. Mou and H. P. Lin, 2013). MSP-SiNPs have high homogeneous porosity, inertness, robustness, thermal stability and high loading capacity, which support them in use multifunctional encapsulation platforms (Cristina Giménez et al., 2015).

Nowadays, there have been various MSP-SiNPs which can be produced. Each of them has their own specific porosity, shape and dimensionality, which are given in Figure 1.2 and Table 1.1 in detail. The most popular and well-defined pore sizes of 2-50 nm is MCM-41, one of MSP-SiNPs. MCM-41 have two dimensional hexagonal pores with the size of 1.5-10 nm. The larger pore sizes are also possible in MSP-SiNPs. SBA-15 can be synthesized with pore sizes of 4.6-30 nm. Three-dimensional pore shape also differs from MCM-41 with two-dimensional pores. FSM-16 is another type of MSP-SiNPs. The structure of FSM-16 looks like MCM-41. However, it is functionally distant from MCM-41. Apart from these MSP-SiNPs, there are various types of MSP-SiNPs, which can be found commercially or synthesized. Some of them with properties are listed in the following table (D. Rath et al., 2014).

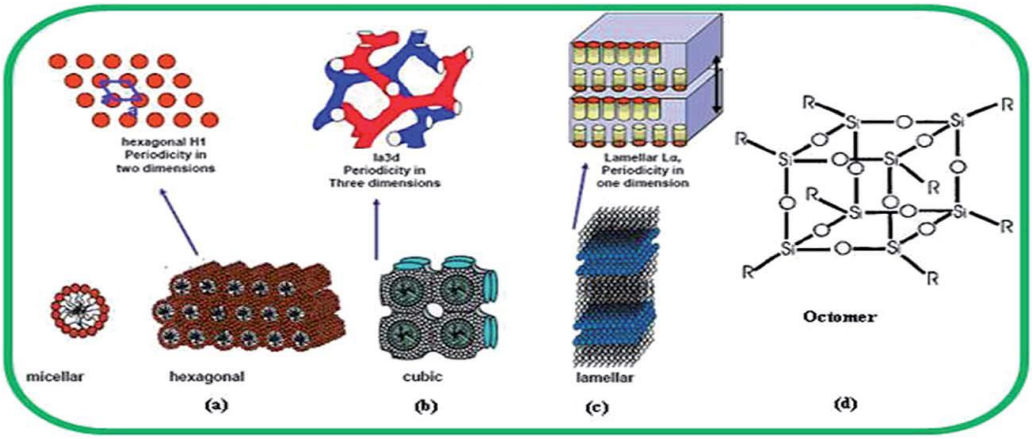

Figure 1.2: Some structures of Mesoporous Silica Nanoparticles. A. MCM-41 with hexagonal dimension. B. MCM-48 with cubic dimension C. MCM-50 with lamellar dimension. D. Octomer dimension

Table 1.1: Various Mesoporous Silica Nanoparticles with properties: dimensionality, unit cell size and mean pore size

SiNP Codes	Dimensionality	Unit Cell Dimensions	Mean Pore Size
MCM-41	2D hexagonal	4.04	3.70
MCM-48	Cubic	8.08	3.48
FSM-16	2D hexagonal	4.38	2.80
SBA-1	Cubic	7.92	2.00
SBA-2	3D hexagonal	5.40;8.70	2.22
SBA-3	2D hexagonal	4.75	2.77
SBA-8	2D rectangular	7.57;4.92	1.87
SBA-11	Cubic	10.64	2.50
SBA-12	3D hexagonal	5.40; 8.70	3.10
SBA-14	Cubic	4.47	2.40
SBA-15	2D hexagonal	11.6	7.80
SBA-16	Cubic	17.6	5.40
HMM	2D hexagonal	5.70	3.10

1.3.1. Functionalization of Silica Nanoparticles

SiNPs are employed with two paths in biosensing technologies (Figure 1.4). In the first way, SiNPs covers other nanoparticles. SiNPs are biocompatible and non-toxic. Thus, toxic and immunogenic effect of the other nanomaterials can be prevented by covering toxic nanomaterials with SiNPs (S. H. Wu, C. Y. Mou and H. P. Lin, 2013). In the second way, SiNPs can be used directly for biosensing technologies. The surface of SiNPs is open to organic functional groups and electrostatic interactions. Dyes or signal generating materials are doped in SiNPs. After biosensing activation, Materials doped in SiNPs produce signals. Dye doped and functionalized with oligonucleotide has served ultrasensitive detection of DNA, 10^4 times higher signal than fluorphore labeled DNA probes (R. M. Kong, X. B. Zhang, Z. Chen and W. Tan, 2011).

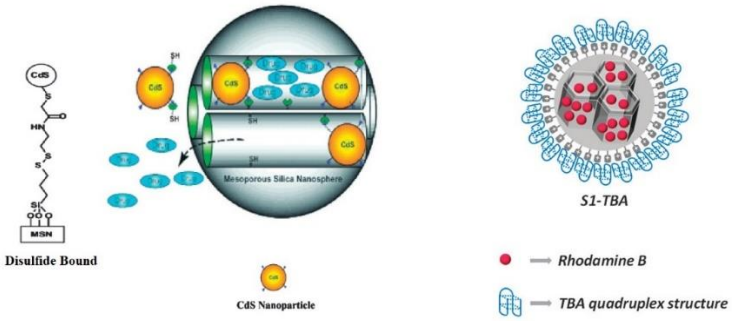

Figure 1.3: Cadmium QDs (CdS) are packed into SiNPs (MCM-41) so that toxicity of cadmium can be prevented. CdS is immobilized on MCM-41 via disulfide bridge (S. H. Wu, C. Y. Mou and H. P. Lin, 2013)**.** Rhodamine B are packed in SiNPs (MCM-41) and functionalization is obtained via electrostatic interaction between aptamer and silane coated surface (Mar Oroval et al., 2013).

The covalent bound of functional groups are mostly constructed by silanes (Zonci Li, Jonathan C. Barnes, Aleksandr Bosoy, J. Fraser Stoddart, Jeffrey I. Zink, 2012). Mostly 3-amiopropyl triethoxysilane, 3-mercaptopropyl trimethoxysilane, 3-aminopropyl trimethoxysilane (APS) and various poly(ethylene glycol)-silanes are used for surface functionalization. These molecules improve silica stability. The linkage types define sensitivity of modification. For example, APS modification is sensitive to pH and light. Acidic environments and UV light break away amino propyl groups, driving to carry packed molecules outside of SiNPs (Alexander Libermana, Natalie Mendeza, William C. Troglerb and Andrew C. Kummelb, 2014). During modification of APS on silica surface, hydroxyl group of silica surface and alkoxyl group of silane are covalently bound (Witucki, 1992). Possible conformations of silica-silane attachment are represented in Figure 1.4.

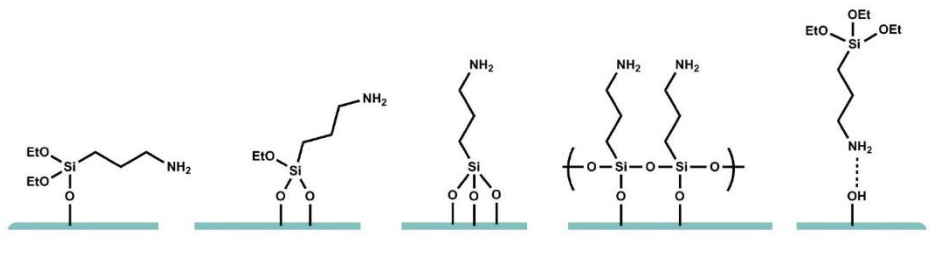

Figure 1.4: The possible binding conformations of APS to SiNPs (Robert G. Acres et al., 2014)

After functionalization of surface, biorecognition material are attached. Some silanes such as N-5-azido-2-nitrobenzoyloxysuccinimide (ANB-NOS) construct covalent attachment with biorecognizer, some of them use electrochemical interactions. In covalent attachment, glutaraldehyde, formation of active ester, sulfhydryl groups on proteins etc. are used for the construction of covalent bonds. Electrical charge is another method to capture antibodies on surface. However, electrical charge changes the conformation of antibodies, causing the decrease in efficiency (Zhan-Hui Wang, Gang Jin, 2003). In the electrostatic interaction, surface coated with silane have positive charge due the presence of NH_3 at neutral pH. Negatively charged nucleic acids or negatively charged other biorecognizers are capable of the construction of electrostatic interaction. In fact, for detection of thrombin, MSP-SiNPs were functionalized with aptamers via electrostatic interaction. The functional SiNPs were tested with human plasma and serum. Limit of detection (LoD) as low as 4 nM thrombin was achieved. (Mar Oroval et al., 2013). The results have indicated that electrostatic interactions on MSP-SiNPs are promising and up-coming.

SiNPs can be loaded with various material for different purpose. Fluorescence dyes, enzymes, active pharmaceutical ingredients, nucleic acids and other nanoparticles can be entrapped in SiNP for biosensensing, drug delivery, gene therapy (Wenzhang Cha et al., 2017) (V. C. Ozalp and T. Schafer, 2011). In biosensing technology, fluorescence dyes are commonly packed in MSP-SiNPs since they can be easily measured and recognized via excitation. Moreover, the lack of excitation light provides them with maintenance of emitting properties. In biosensing and showing release kinetics, fluorescence dyes are measurable after uncapping SiNPs (E. Climent et al., 2010). Other nanoparticles can be packed in SiNPs. SiNPs is nonimmunogenic and inert materials so immunogenic nanoparticles and reducible or oxidable material can be prevented in SiNPs by coating (S. H. Wu, C. Y. Mou and H. P. Lin, 2013) (X. Wang, R. Niessner, D. Tang and D. Knopp, 2016). Loaded, functionalized and capped SiNPs need to be placed in some platform to work well such as micro fluidic systems or lateral flow platforms for biosensing technologies.

1.4. Lateral Flow Assay

Development of nanomaterials in biosensing technologies made paper based biosensors advantageous. In the developed countries, gas chromatography mass spectrometry, ultra-high-performance liquid chromatography tandem mass spectrometry, high pressure liquid chromatography, Enzyme -Linked Immunsorbent Assay (ELISA) etc. have been mostly used with high sensitivity and specificity for detection of small molecules. However, people in undeveloped countries cannot approach these methods. By carrying nanomaterials into paper based biosensors including Lateral Flow Assays (LFAs), LFAs have been gaining advantageous as substitute methods in real samples (E. B. Bahadır and M. K. Sezgintürk, 2016). Thanks to short notice assay, low cost, friendly user formats and actualizing ASSURED request, LFAs have attracted interest. Application of nanomaterials in detection of proteins, nucleic acids, whole cells and other biocompounds has served fascinating results to LFA technology (Daniel Quesada Gonzalez, Arben Merkoçi, 2015). Moreover, LFAs offer Point of Care (PoC) testing in which there is not any complicated machine and it can be performed in everywhere patients are. Even though, LFAs pose benefits during manufacturing and application, it has some drawbacks. Both benefits and drawbacks are listed on Table 1.2.

Table 1.2: Benefits and drawbacks of Lateral Flow Assays (LFAs) (Katarzyna M. Koczula, Andrea Gallotta, 2016)

Benefits	**Drawback**
• Facile preparation of device	• Qualitative or semi-quantitative
• Low-cost	• Reproducibility depends on many variables
• Simple and user friendly	• Low signal intensity
• Requirement of small amount of sample	• Weak quantitative discrimination
• High potential to commercialization	• Pre-treated sample
• Applicable without trained people	
• Portable detection device	
• Rapid Diagnosis	

LFAs just needs basic four components: sample pad, conjugate pad, reaction membrane and absorbent pad. It is expected that sample pad cannot interact with sample during application. Cellulose acetate and glass fiber membrane have low affinity to proteins. Thus, the sample pad is generally made from cellulose acetate and glass fiber membrane. Absorbent pad keeps the flow of liquid on conjugate pad and reaction membrane by supporting capillary force towards the end of LFA strip. Conjugate pad carrying functionalized nanomaterials binds to target molecule and run along a chromatography strip with controlled rate. The crucial constructive material of LFA is nitrocellulose membrane, or reaction membrane. Nitrocellulose membrane includes test line and control line so it should provide with good binding to capture probes. Nitrocellulose membrane includes strong dipole of nitrate ester which interacts with the peptide bonds of antibodies and via electrostatic interaction antibodies can be fixed on nitrocellulose membrane (M. J. Raeisossadati, N. M. Danesh and F. Borna, 2016) (E. B. Bahadır and M. K. Sezgintürk, 2016).

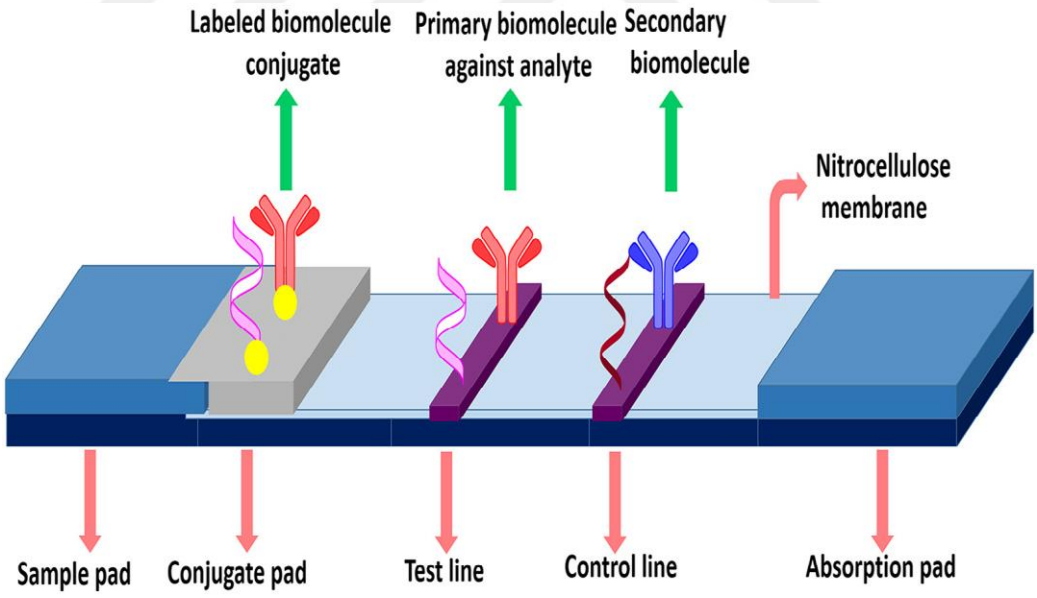

Figure 1.5: Representation of Lateral Flow Assay (LFA) components (E. B. Bahadır and M. K. Sezgintürk, 2016)

1.4.1. The Classification of Lateral Flow Assays

LFAs are used for detection of proteins, haptens, nucleic acids and amplicon. However, its classification is based on functionalization. The description of biorecognizing molecule defines the type of LFAs as Antibody Based Lateral Flow Assays and Nucleic Acid Based Lateral Flow Assays (K. M. Koczula and A. Gallotta, 2016).

1.4.1.1. Antibody Based Lateral Flow Assays

As a biorecognition molecules, antibodies are employed on test line and control line. These LFAs are also called as Lateral Flow Immuno-Assays (LFIAs) Primary monoclonal antibody interacts with its own antigen, which is target. Both constitute immunocomplex. Secondary monoclonal antibody binds to primary antibody or immunocomplex. Sandwich method and competitive method are two methods in the construction of Antibody Based LFAs (R. Kumar, C. K. Singh, S. Kamle, R.P. Sinha, 2010).

1.4.1.1.1. Sandwich Format Lateral Flow Assays

In this system, three varied antibodies are immobilized on LFAs' platform. Firstly, labelled antibody which was attended to conjugate pad and specifically binds to epitope of target antigen. The labelled antibody can be called as reaction antibody. Due to capillary flow force and rehydration, reaction antibody flow to control line and test line. Control line includes second antibody, called as detection antibody which interacts with second epitopes of target antigen. In the presence of target antigen, both reaction antibody and detection antibody form sandwich. They can generate signal on test line. On control line, secondary antibody detects reaction antibody and produces signal to show whether the system works (J. Singh, S. Sharma, S. Nara, 2015).

1.4.1.1.2. Competitive Format Lateral Flow Assays

Small molecules with low molecular weight are not able to bind two antibodies. By following competitive format, they can be detected. Labelled antibody is placed onto conjugate pad while test line includes analyte carrier molecule. Control line has secondary antibody. Antigen target and analyte carrier try to bind primary labelled antibody in a competitive format. In the presence of target antigen, the color seems on control line while the lack of target antigen causes the color to appear on both lines (B. Ngom, Y. Guo,Wang X, Bi D., 2010).

1.4.1.2. Nucleic Acid Based Lateral Flow Assays

Recently nucleic acids have been employed for biofunctionalization of nanoparticles on LFAs. Nucleic acid can be used for detection of nucleic acids or protein. Nucleic acid based lateral flow assays are created by two ways: antibody dependent and antibody independent. In antibody dependent LFAs, the interaction between double stranded amplicon and nucleic acid-antibody is constructed. To identify a specific sequence, primers with different tags are used. The tag specific antibody is placed on nitrocellulose membrane so that it can interact with target and nanoparticle. Visualization can occur on nitrocellulose membrane. In antibody-independent LFAs, binding properties of amplicon and probe construct the principle of assay. Both amplicon and probe are labelled and they bind to each other irreversibly. Visualization is seen on nitrocellulose membrane (E. B. Bahadır and M. K. Sezgintürk, 2016).

Nucleic acids have been thought as potential substitute of antibodies in biosensors since they also have similar recognition properties. In fact, nucleic acids are superior because they have small size, high stability, non-immunogenicity, the ability of penetrating to tissue. The comparison of nucleic acids and antibodies are listed on following table (A. Chen and S. Yang, 2015).

Table 1.3: Comparison of nucleic acids with antibodies for biosensors

Oligonucleotides	**Antibodies**
• Lack of immunogenicity	• Difficult for nonimmunogenic
• In vitro selection under various conditions	• Restricted conditions due to animal immunization
• Efficient chemical synthesis with low cost	• Time-consuming with high cost
• Uniform in batch activity	• Varied in batch activity
• Long shelf life with transportation tolerant	• Short shelf life with requirement of cold chain
• Low detection limits between nanomolar to picomolar	• Low detection limits between nanomolar to picomolar
• Easy and cheap modifications	• Difficult and expensive modifications

Single stranded (ss) DNA or RNA oligonucleotides have the ability of binding to metal ions, small organic molecules, proteins and even complete cells. The type of ssDNA with high and specific affinity to proteins and other molecules are called as Aptamer (R. M. Kong, X. B. Zhang, Z. Chen and W. Tan, 2011). Aptamers are generally in length 10 to 100 bases with typical structural motifs including three-dimensional folding such as internal loops, purine rich bulges, hairpin structures etc. (A. Chen and S. Yang, 2015).

Single stranded Nucleic Acids sensing methods are highly sensitive and do not require labelling systems. Single stranded probes without conformational changes can be used for detection of nucleic acids according to Watson-Crick pairing. ssDNAs or ssRNAs are immobilized on recognition sites. The binding of target molecules causes to open gates and stimulate and generate signals. The dynamics of target capture is known and predictable. Thus, inherent affinity against target DNA can be maintained. During signal propagation (T Gregory Drummond, Michael G Hill, Jacqueline K Barton, 2003).

The linkage between the probe and immobilization matrix should be prevented from affecting chemical properties of DNA. Several immobilization methods have been introduced up to now such as electrochemical adsorptions (Kavita Arora, Subhash Chand. D. Malhotra , 2006) and entrapment methods and covalent bindings. Electrochemical methods are simple but they generate weak interaction

between probe and immobilization matrix. Negatively charged nucleic acid backbone is generally linked to positively charged surface. The presence of complementary sequence causes to hybridization. However, biosensors with electrochemical interaction have short shelf life and low stability of biosensors since the electrochemical linkage can be easily disrupted. On the other side, covalent linkage seems to be more strict and stable, compared with electrochemical interactions. One end of probe is mostly attached to immobilization matrix. The other end is free for hybridization. Target DNA forms double stranded DNA by hybridizing with single stranded probe (Alizar Ulianas, Lee Yook Heng, Sharina Abu Hanifah and Tan Ling Ling, 2012).

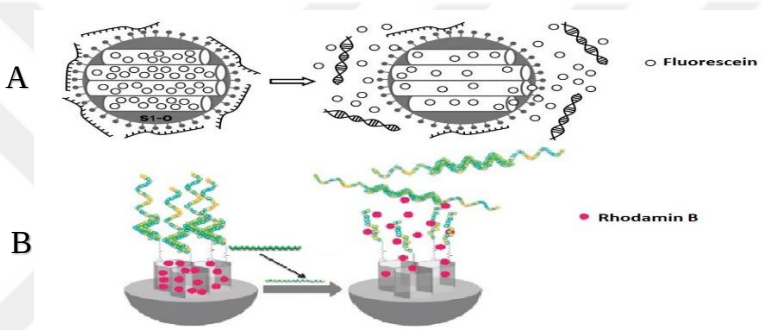

Figure 1.6: A. Electrochemical binding of probes (E. Climent et al., 2010) **B.** Covalent binding of probes (Luis Pascual et al., 2014)

In LFAs, to get PoC testing, the signal is required to be seen without complex equipment so the result should be visible to the naked eyes. Colorimetric reactions on LFAs have been getting popularity. Hybridization based LFAs take in colorimetric reactions.

1.4.2. Colorimetric Sensors in LFAs

The paper based devices are mostly combined with colorimetric detection systems. The combination enables PoC for target DNA, RNA and other target analytes. Determination of target occurs via change on color due to signal- analyte interaction. Without complex equipment, the results can be obtained in a fast manner around patients. Thus, PoC testing methods generally focus on colorimetric analysis (Qingkun Kong, Tanhu Wang, Lina Zhang, Shenguang Ge,

Jinghua Yu, 2016). In PoC testing, quantification of signal is not required but the change on color can be measured and analyzed via the RGB color differences (Tamaki Soga, Yusuke Jimbo, Koji Suzuki and Daniel Citterio, 2013). Fluorophores or colorimetric reactions can be employed in colorimetric sensors. Fluorophores are entrapped in biosensors. The presence of target cause to the release of fluorophores (E. Climent et al., 2010) (Luis Pascual et al., 2014). By this way, signal can be recorded. In Figure 1.7, cargos are fluorophore.

Colorimetric reactions are used in colorimetric assays. In colorimetric assays, the presence of analyte stimulates the colorimetric reaction, which are mostly redox reactions. 3,3′,5,5′-Tetramethylbenzidine (TMB) - Horseradish Peroxidase (HRP) – Hydrogen Peroxide (H_2O_2) system is accommodated in these systems (Yujun Song, Konggang Qu, Chao Zhao, Jinsong Ren, and Xiaogang Qu, 2010). Benzidine and its derivatives are most common substrate for HRP. Aromatic amines of TMB are oxidized in the presence of H_2O_2. The oxidation occurs in two steps. In the first step, one electron oxidation product, cation free radical, appears in blue color. This intermediate cation free radical can be detected at 370 or 652 nm of wavelength. In the second step, the reaction is completed and diimine is formed because of the second electron transfer. Diimine appears in yellow color with 450 nm of wavelength (P. D. Josephy, T. Eling and R. P. Mason, 1982).

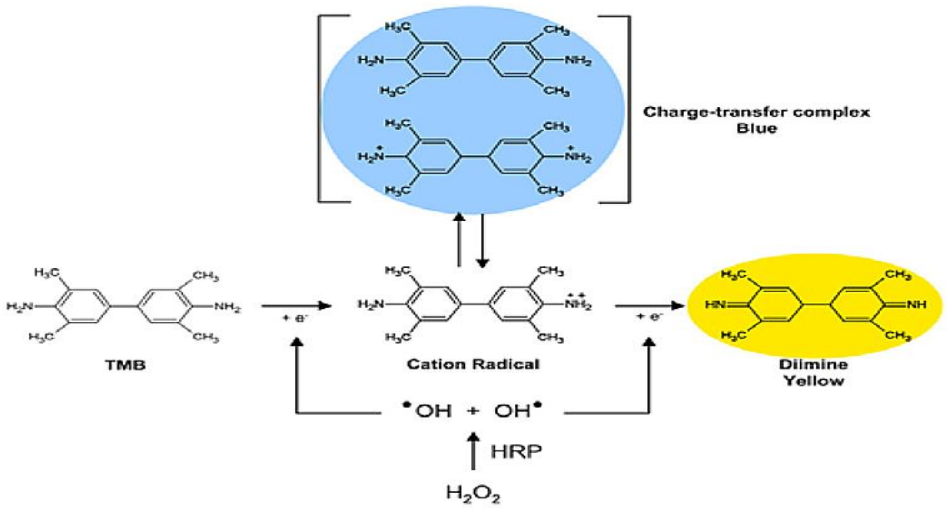

Figure 1.7: Chemical structure of TMB and its oxidation products (Nebraska Redox Biology Center Educational Portal, 2017).

1.5. Foodborne Diseases

The increasing food demand has been raising difficulties in food safety. During manufacturing, transportation and consumption, foods are always at risk of contamination. The disease coming from contaminated food is defined as foodborne disease. 600 million (95% uncertainty interval [UI] 420–960 million) people suffered from foodborne disease in 2010. In other words, one in each ten people almost got sick due to food contamination. 420,000 (95% UI 310,000-600,000) people passed away after consumption of contaminated foods. Unfortunately, 40% people suffered from foodborne disease is solely just children under 5 years old (WHO, 2015). Up to now, many contaminants have been found and described in World Health Organization: pesticide and veterinary drug residues, endocrine disrupters, food additives, packing materials, environmental contaminants (dioxins and heavy metals), and contaminants of natural origin (WHO, 2015).

Centers for Disease Control and Prevention (CDC) categorizes foodborne illnesses into two groups, unspecified agents and known food pathogens. Laboratory based data help to evaluate foodborne disease trends and to take precaution against foodborne diseases. However, most portion of foodborne disease cannot be defined. Some acute gastroenteritis agents may not be estimated due to the paucity of data and are involved in unspecified agents. Agents (microbes, fungi, metals, biotoxins, organic toxins) cause acute diseases. Self-healing brings about the lack of data on diseases. Additionally, most of foodborne pathogens were discovered in a recent decade. There could have been remained and undefined pathogens waiting for being identified (Elaine Scallan, Patricia M. Griffin, Frederick J. Angulo, Robert V. Tauxe, Robert M. Hoekstra, 2011).

As known food pathogens, 31 major pathogens were described (Elaine Scallan et al., 2011). Some of these pathogens are norovirus, *Salmonella* species (spp.), *Clostridium perfringens*, and *Campylobacter* spp. Foodborne threats pose different progress of illness with various symptoms and signs such as Diarrhea, abdominal cramps, vomiting, fewer. Information about progress of some

foodborne illnesses is stated in the following table. Concerning hospitalization, *Salmonella* spp. occupy the biggest percentage, 35%, among major pathogens. Also, *Salmonella* spp. are the most mortal agents among them. In other words, *Salmonella* is prominent and major pathogen among foodborne pathogens.

Table 1.4: Foodborne disease-causing organisms with their own sign and symptoms, required time for progress of illness, duration of disease and transmission source (FDA, 2016).

Organisms	Onset Time After Ingesting (Hour)	Signs and Symptoms	Duration (Day)	Food Sources
Salmonella	6-48	Diarrhea, Fever, Abdominal Cramps, Vomiting	4-7	Eggs, Milk Products, Raw Fruits, Vegetables, Water
Noroviruses	12-48	Nausea, Vomiting, Abdominal Cramping, Diarrhea, Fever, Headache	1-5	Drinking Water, Uncooked Foods and Cooked Foods
Clostridium perfringens	8-16	Intense Abdominal Cramps, Watery Diarrhea	1	Meats, Poultry, Gravy, Dried or Precooked Foods
Campylobacter jejuni	48-70	Diarrhea, Cramps, Fever, Vomiting	2-10	Raw and Undercooked Poultry

1.5.1. Salmonella

The most mortal agent of foodborne disease is *Salmonella*, the disease of which is known as salmonellosis. The name of the genius *Salmonella* was derived from pathologist Daniel Elmar Salmon who firstly signed it in a well-studied group of organisms (Cooke, 2007). It is involved in *Enterobacteriaceae*, known as enteric bacteria living in the gastrointestinal system of warm blood animals, but they do not have the ability to ferment lactose and sucrose when hydrogen sulfide and gas are released (Arvid, 2016). It is a rod shaped (bacilli), gram negative, non-spore forming, facultative anaerobic bacterium. It has peritrichous flagella providing motility (Figure1.8). On average, Salmonella is 2-5 microns long to 0.5-1.5 microns wide. (Dougnon, 2016).

Figure 1.8: The image of *Salmonella* bacterium on Transmission Electron Microscope with 13,250 magnifications. Stringy like structures projecting in all directions are called as peritrichous flagella providing to motion (Brands, 2006).

Salmonella spp. are so resilient to adapt extreme environmental condition. Optimum temperature can be thought between 35-37ºC but some of serotypes can survive at 54ºC and multiply at 2ºC. Its optimum pH is in the pH range of 6.5 and 7.5. However, they can stay alive between pH 4-9.

1.5.1.1. Classification and Nomenclature

To classify serotypes of *Salmonella*, flagellar (H) antigens, somatic (O) antigens, virulence (Vi) capsular (K) antigens were employed which was accepted by the International Association of Microbiologists in 1934. In this system, each serotype was species. Kauffmann-White scheme classified *Salmonella* spp. by checking antigens. If this system were valid today, 2643 *Salmonella* spp. would be defined. However, a phylogenetic tree based classification is valid. 2463 serotypes were analyzed with the phylogenetic construction. *Salmonella enterica* (2443) and *Salmonella bongori* (20) was defined as species, according to World Health Organization (WHO) Collaborating Centre and Disease Control and Prevention (CDC) (Pui, 2011) (Brenner, 2000).

Salmonella enterica includes six subspecies, which are represented with roman number; I (*enterica*), II (*salamae*), IIIa (*arizonae*), IIIb (*diarizonae*), IV (*huotenae*) and VI (*indica*). Among these subspecies, only *S. enterica* subspecies I cause disease in warm blood animals (Porwollik, 2004). *S. enterica* subspecies I consist of many serovars. Even though, more than 2300 serovars has been identified, just 50 of them are defined as human pathogen. All of 50 serovars are found at *S. enterica* subspecies *enterica*. Some of these pathogen serovars are typhi, paratyphi A, paratyphi C, enteriditis, sendai (Uzzau, 2000). The remained serovars belongs to the other subspecies of *S. enterica* and *S. bongori* and are commonly obtained from cold blood animals and environment. *Salmonella bongori* is also called as subspecies V. Similarly, it can be found in environment and cold blood animals (Brenner, 2000).

1.5.1.2. Epidemiology and Clinical Presentation of Salmonella

Salmonellosis is defined as the disease coming from *Salmonella* spp. Each year, tens of millions of humans suffers from salmonellosis and more than hundreds of deaths are reported every year. At the beginnings of 1990s, the usage of antimicrobials made bacteria resistant to antibiotics and other drugs, which caused serious problem in public health (WHO, 2013). The report of WHO in 2015 stated that salmonella with its own various types was observed as the one of the greatest foodborne burden. 8.76 million DALYs (disabled adjusted life year) (95% UI 5.01–15.6 million) came from salmonella infections (WHO, 2015). In 2013, it was stated in the common report of EFSA (European Food Safety Authority) and ECDC (European Center for Disease Prevention and Control) that 82,694 salmonellosis incidences were confirmed per 100,000 population of 32 European countries (EFSA and ECDC, 2016).

Salmonella enterica subspecies *enterica* (I) causes the most of salmonellosis. However, in clinical view and concerning characteristics of illness, serotypes of subspecies I are divided into Typhoidal *Salmonella* and Nontyphoidal *Salmonella* (Ohad Gal-Mor, Erin C. Boyle, and Guntram A. Grassl, 2014). Typhoidal *Salmonella* is carried with human feces contaminated food and water. Low and

middle-income countries or undeveloped countries are under the risk of Typhoidal *Salmonella* since they do not have well working sanitation and food safety systems. After establishing the infection, acid secretion is suppressed and acute enteric fewer is seen in the internal ileum. (Khosla, 1993). Generally, illness seems mild disease so self-medication as hospital out patients can be chosen. Thus, some cases unfortunately cannot be considered in epidemiologic studies. Sustained fewer (39-40^{o}C), chills, anorexia, dry cough, sore throat, malaise, frontal headache are also seen during illness. (John A. Crump, Maria Sjölund-Karlsson, Melita A. Gordon, Christopher M. Parrye, 2015) (Ohad Gal-Mor et al., 2014). Nontyphoidal Salmonella, opposite of typhoidal one, seems in industrialized, developed and developing countries since agents are transmitted through commercial products. Commercial foods are contaminated by animal feces and drive to self-limited enterocolitis and diarrhea. Immunocompromised people such as infants, young children and the elderly can fall serious disease with diarrheal enterocolitis and bloodstream infections. Clinical diagnosis is challenging without laboratory facilities. After 6-72 hours' incubation, nausea, vomiting, abdominal pain, watery and sometimes bloody diarrhea can be symptoms. In the compromised host, these symptoms can be maintained for several weeks while healthy host can manage to recover within 2-7 days (Chiu, 2010).

1.5.1.3. Diagnosis of *Salmonella*

Diagnostics tests are especially required for iNTS (invasive nontyphoidal salmonella) due to indistinguishable symptoms. Diagnosis of Typhoidal *Salmonella*, on the other side, is critical for public health assessment. Various tests and different biological samples are used in salmonella diagnosis. Their success and effectivity depends on agents, host and illness period. Bacterial culture, serological assays and molecular assays are common diagnostic methods (John A. Crump et al., 2015).

Bacterial culture is generally carried out with sterile blood and bone marrow aspiration. Generally, 48 hours is enough to find the positive cultures and after five days, almost all cultures can be positive. Following passage, subcultures are

used for biochemical tests, agglutination with antisera in identification of serovars. Even though, the blood culture has low sensitivity (40%), bone marrow culture shows the highest sensitivity among all diagnostic methods. However, bone marrow culture requires well educated personnel and specialized and sterile equipment. Also, there are other specimens for culture such as stool (gaita), rectal swab (Jason R. Andrews, Edward T. Ryan, 2015).

In Serological Assays: several monoclonal antibodies such famous ones against LPS (O), Flagellar (H), Vi capsular polysaccharide and outer membrane (OMP) antigens are employed in agglutination tests (widal test), Enzyme-Linked ImmunoSorbent Assays (ELISA), Sodium dodecyl sulfate polyacrylamide gel electrophoresis (SDS-PAGE) immunoblotting etc. Sensitivity and specificity of serologic assays, based on antigen detection, is regarded as moderate in plasma and urine. Additionally, among results coming from acute sample, false-negative and false positive results are common (John A. Crump et al., 2015).

As molecular assays, nucleic acid amplification tests such as conventional PCR, real time PCR, nested PCR, LAMP (loop mediated isothermal amplification) are employed in diagnosis of salmonella. Molecular assays can detect small number of organisms, unculturable organisms and death organisms. While their specificity is excellent, their sensitivities rely on the designed primers, probes and specimens. Human DNA or other contaminate DNA disrupts sensitivity. It has high specificity. Molecular assays have almost perfect specificity however they require well equipped laboratory and trained personnel (Jason R. Andrews, Edward T. Ryan, 2015).

Table 1.5: Conventional diagnosis methods of Salmonellosis with their own example assays, sensitivity, specificity, required time, laboratory requirements.

Class	Example Assays	Sensitivity	Specificity	Time to Results	Requirements
Bacterial Cultures	Blood Culture Bone Marrow Culture	Low	Excellent	1-5 days	moderate
Serologic Assays	*ELISA,* *SDS-PAGE immunoblotting* *Widal* *RTI*	*Low moderate*	*Moderate*	*1-3 hours*	*moderate*
Molecular Assays	PCR LAMP Proteomics	Variable	Excellent	1-3 hours	high

Salmonella can invade the cultured epithelial cells via *InvA, B, C, D* genes. *InvA, B, C* locate on same transcriptional unit while *InvD* locates on the other unit. Thus, *InvA, B, C* use same operon which is called as the *invABC* operon. Without *InvA*, the ability of invasion disappeared according to the report of Galan in 1992. The presence of *InvA* gene was confirmed in most serotypes of *Salmonella* so *InvA* gene can be accepted as *Salmonella* specific gene. During molecular detection, *InvA* gene was used in a molecular detection method, PCR. Certain PCR products of *InvA* gene has been evaluated in detection of *Salmonella* serotypes (Rahn K, De Grandis SA, Clarke RC, McEwen SA, Galán JE, Ginocchio C, Curtiss R, Gyles CL., 1992).

1.6. Aim of the Study

Salmonellosis is a fatal disease in undeveloped and developing countries. Even though, there are various conventional diagnosis methods for Salmonellosis, concerning time, cost, sensitivity and specificity, these methods are insufficient because of the presence of their high-cost demands and skilled person needs high-requirements. LFAs have been presenting promising and up-coming efficiency for diagnosis purpose. Thus, in this study, the development of a novel LFA with low cost, user friendly, high specificity and sensitivity was aimed for diagnosis of *Salmonella* by detecting its amplicon with specific sequences.

CHAPTER 2

MATERIALS AND METHODS

2.1. Materials:

2.1.1. Chemicals

All chemicals used in this study were analytical grade and obtained from Sigma-Aldrich, Merck, AppliChem. All water in the experiments were ultrapure one with 18.2 MΩcm resistance

2.1.2. Solutions and Buffers

The preparation of solutions and buffers with their compositions were described in Appendix A

2.1.3. Oligonucleotides

Oligonucleotides as probes and primers for PCR amplification were ordered from Integrated DNA Technologies (IDT) with HPLC purification. Two probes, Probe-1 and Probe-2 includes complementary sequences to *InvA* gene. Probe-1 is the components the region at the 5' end of PCR products while Probe-2 was in the middle of PCR product. The other probe, uncomplementary probe, was designed with uncomplementary sequence for *InvA* gene.

Synthetic targets sequences were purchased from Oligomer Biotechnology with standard desalting. Target-1 was designed to be complementary to Probe-1 while Target-2 was complementary to Probe-2. Control target did not include any complementary sequence to any of the probes.

As a target, 284 bp amplicon was obtained from *InvA* gene, coming from *S. typhimirium* by applying PCR with *InvA* primers. The amplicon included complementary sequences to Probe-1 and Probe-2. As a negative control target, 292 bp amplicon without any complementary sequence was obtained from *ycdT* gene of *Escherichia coli* DH5 alpha. The sequences of primers, probes and synthetic targets were given in the following table 2.4.

All probes, primers and synthetic targets were resuspended in sterile nuclease free water without additional purification steps and stored at -20^{o}C. Stock solution of primer with 100 μM, stock solution of synthetic targets with 100 μM and stock probes solutions with 5000 μM were prepared. Working solutions were prepared from these stock solutions.

Table 2.1: Sequences of primers for 284 bp amplicon produced from *InvA* gene

Primers	**Sequence**
***InvA* Forward Primer**	5'- GTG AAA TTA TCG CCA CGT TCG GGC AA-3'
***InvA* Reverse Primer**	5'-TCA TCG CAC CGT CAA AGG AAC C-3'

Table 2.2: Sequence of primers for *ycdT* gene of *E.coli* DH5 *Alpha*

Primers	**Sequence**
***ycdT* Forward Primer**	5'- AGC ATA CGA CCA GAT GAC CTT T -3'
***ycdT* Reverse Primer**	5'- CAT CCC TCA CAA CCA CCT TAT TAC -3'

Table 2.3: Sequences of probes which were used in silica functionalization

Probes	**Sequence**
Probe-1	5'-CCA ATA ACG AAT TGC CCG AAC GTG GCG ATA ATT T-3'
Probe-2	5'-TAA CGA TAA ACT GGA CCA CGG TGA CAA TAG AGA A-3'
Uncomplementary Probe	5'-TAT GGT GTA GGT CGA GGC AGG TGT TTG CAG TCA G-3'

Table 2.4: Sequences of synthetic targets in which synthetic target-1 is complementary to Probe-1 and synthetic target-2 is complementary to Probe-2.

Synthetic Targets	Sequence
Synthetic Target-1	5'-AAA-TTA-TCG-CCA-CGT-TCG-GGC-AAT-TCG-TTA-TTG-G-3'
Synthetic Target-2	5'-TTC-TCT-ATT-GTC-ACC-GTG-GTC-CAG-TTT-ATC-GTT-A -3'
Control Target	5'-GGT-CAG-GTC-TGG-GTA-AAA-ATG-TCA-AGC-GGT-AGG-T-3'

2.1.4. Bacterial Strain.

Sallmonella enterica seroytpes *Salmonella* typhimurium (ATCC 14028), *Salmonella* enteritidis (ATCC 13076), and *Salmonella* infantis and *Escherichia coli* strain DH5α were kindly provided from NANObiz Ltd. Co., Ankara, TURKEY.

2.1.5. Silica Nanoparticle

Mesoporous (MSP) silica nanoparticles (SiNPs) were purchased from Sigma-Aldrich (USA). SNPs was in powder form with 2.1-2.7 nm pore size. Each unit of SiNPs were stated to be 4.5-4.8 nm in product details.

2.1.6. Components of Lateral Flow Assay Platform

Lateral flow Assay (LFA) platform was constructed with sample pad, absorbent pad and nitrocellulose membrane. Hi-Flow nitrocellulose membrane card and sample/absorbent pads (SureWick®name) were purchased from Millipore, Germany. HF180 and HF240, Hi-Flow^{TM} Plus nitrocellulose membranes were used. Respectively, their capillary flow rates are 180 ± 45 (sec/4cm) and 240 ± 45 (sec/4cm). Nitrocellulose membranes are packed as 6 cm X 30 cm (± 0.05 cm). Sample pad and absorbent pad are porous materials and they create the flow of the sample on nitrocellulose membrane.

2.2. Methods

2.2.1. Preparation of Target

2.2.1.1. Synthetic Target Preparation

Synthetic targets were dissolved in DNA/RNA free water as stock concentrations of 100 μM. They were used for assay and Limit of Detection (LoD). Similarly, control target was prepared and obtained working solution with 10 μM.

2.2.1.2. Amplicon Target Preparation

2.2.1.2.1. Isolation of *Salmonella* Genomic DNA

Before isolation of *Salmonella* genomic DNA, *Sallmonella enterica* seroytpes *Salmonella* typhimurium, *Salmonella* enteritidis, and *Salmonella* infantis were grown in Tryptic Soy Agar (TSA) for 16 hours at 37^{o}C. The colony was picked up to Tryptic Soy Broth (TSB) and was incubated for 16 hours at 37^{o}C in rotary shaker (100 rpm). To use as control, *Escherichia coli* strain DH5α was grown in Luria Bertani Agar (LBA) for 16 hours at 37^{o}C and its colony was taken onto Luria Bertani Broth (LBB). The incubation was carried out for 16 hours at 37^{o}C within rotary shaker (100 rpm). Their genomic DNA were isolated by using NANObiz DNA4U Bacterial Genomic DNA isolation kit. Before last centrifugation, as an additional step to protocol, columns were kept at 65 ^{o}C for 5 minutes. These obtained genomic DNAs were used as a template in Polymerase Chain Reaction (PCR). The amount of genomic DNA was quantified by using NanoDrop 2000 spectrophotometer (Thermo Scientific,USA).

2.2.1.2.2. Polymerase Chain Reactions

The components of PCR with their own amount and concentrations were shown on the following tables for 284bp, (*Sallmonella enterica* seroytpes*) and ydcT* (*Escherichia coli* strain DH5α).

Table 2.5: The optimized amount of PCR components in 50 µL for 284bp (Target Amplicon)

Reagents	1 RXN (µL)
dH_2O	33.1
10X buffer	5
25 mM $MgCl_2$	4
10 µM F. Primer	2
10 µM R. Primer (1)	2
10 mM dNTP	1.5
Taq Pol	0.4
DNA template (10ng/µL)	2
Total volume	50

Table 2.6: Optimized temperatures of PCR cycles for 284 bp PCR products (Target Amplicon)

Steps		Temperatures	Duration
Initial Denaturation		95°C	2 Minutes
40 cycle	**Denaturation**	95°C	30 Seconds
	Annealing	64°C	30 Seconds
	Extension	72°C	30 Seconds
Final Extension		72°C	4 Minutes

Table 2.7: The optimized amount of PCR components in 50 µL for *ycdT* (Control Amplicon)

Reagent	1 RXN (µL)
dH_2O	34.6
10X buffer	5
25 mM $MgCl_2$	4
10 µM F. Primer	1.25
10 µM R. Primer (2)	1.25
10 mM dNTP	1
Taq Pol	0.4
DNA template	2.5
Total volume	50

Table 2.8: Optimized temperatures of PCR cycles for *ycdT* (Control Amplicon)

Steps		Temperatures	Duration
Initial Denaturation		95ºC	5 Minutes
40 Cycle	**Denaturation**	95ºC	30 Seconds
	Annealing	54ºC	30 Seconds
	Extension	72ºC	30 Seconds
Final Extension		72ºC	4 Minutes

2.2.1.2.3. Agarose Gel Electrophoresis

50 mL of 1.5% (w/v) agarose gels with 5 µL of Ethidium bromide (5mg/mL) were used for visualization of all amplicons. 1.5 gram of agarose was completely dissolved in 100 mL of 1X TAE (pH 8.3) via microwave heating. After cooling, 5 µL of Ethidium bromide (5mg/mL) was added into gel solution. The solution was poured into a gel tray. By getting rid of bubbles, comb was placed into the tray. After solidification of the gel, the comb was removed and the gel was set down in an electrophoresis tank within 1X TAE. Amplicons was loaded with 6X loading dye (Thermo Scientific, USA). DNA ladders, previously mixed with 6X loading dye, were also loaded into wells. 100V for 30 minutes was applied to the gel. The gel was visualized by UV acquisition system.

2.2.2. Preparation of Silica Nanoparticles

2.2.2.1. Entrapping TMB into SiNPs

Benzidine is a common substrate for HRP-H_2O_2 oxidation. In this study, 3,3',5,5'-Tetramethylbenzidine (TMB) (Sigma-Aldrich, Germany) was entrapped in SiNPs firstly. As a stock solution, 1M of TMB was prepared by dissolving TMB in Dimethyl Sulfoxide (DMSO). As a working solution, 0.2 M, 0.5 M were also prepared from stock TMB solution. 2.5 mg of SiNPs were suspended in 495 µL of 1X PBS. SiNPs solution was sonicated for 5 minutes. 5 µL of working 5 Mm TMB solution was added. After vortex mix, TMB-SiNPs were incubated overnight in 2D shaker (Heidolph DuoMax 1030).

2.2.2.2. Silanization of TMB-SiNPs

After overnight incubation of SiNPs with TMB, TMB-SiNPs were centrifugated at 6000 rpm for 5 minutes (MPV-65R). Supernatant was discarded and pellet was suspended again with 475 µL of 1X PBS and 25 µL of 3-Aminopropyl-trimethoxysilane (APS) was added for silanization. APS-SiNPs were incubated at 37 ^{o}C for 3 hours in 2D shaker (20 rpm). APS chemically binds to surface. Amino group of APS accommodates on surface of SiNPs.

2.2.2.3. Capping SiNPs with Oligonucleotide Probes

Silanized SiNPs were centrifugated at 6000 rpm for 5 minutes and dissolved again with 500 µL of 1X PBS. Silanized SiNPs were separated into 5 tubes. Each aliquot had 100 µL of TMB-SiNPs solution. Again TMB-SiNPs were centrifugated at 6000 rpm for 5 minutes. Supernatant was discarded. 10 µL of 100 µM oligonucleotide probe was added onto pellet and 10 µL of 1X PBS was added. For creating null SiNPs, milliQ was used instead of probe and 10 µL of MilliQ was added. The mixture was incubated at 37 ^{o}C for an hour in shaker. At the end of incubation, lid of tubes was opened and overnight dried at room temperature. After silanization, surface could accept oligonucleotide probes via ionic interaction with negatively charged phosphate backbone of oligonucleotide.

2.2.3. Preparation of Lateral Flow Assay Platform

The platform of LFA consists of three parts in this study: sample pad, absorbent pad and nitrocellulose membrane. Sticky ends of nitrocellulose membrane at both sides were covered. Sticky coverings were removed and sample pad and absorbent pad were fixated at the ends of nitrocellulose membrane. These constructed LFA cards were cut into 3mm width. Functional SiNPs were placed onto LFA platform 4 mm away from sample pad. Following SiNPs, HRP was placed onto LFA platform 2 mm below SiNPs. The arrangement of LFA platform was represented below Figure 2.1.

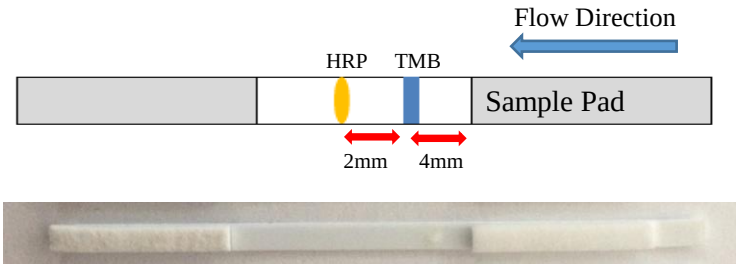

Figure 2.1: Organization of Lateral Flow Assay Platform.

2.2.4. Treatment of Samples on LFA

As a sample, synthetic targets and amplicons were used. Synthetic targets are already single stranded so they could be directly used. On the other hand, amplicons are double stranded. To enable hybridization of amplicon with probes, amplicons had to get single stranded. Thus, at 95 ^{o}C for 4 minutes, amplicons were incubated and they were immediately carried into icebox so that double strand construction and other formation could be prevented. For each strip, 26 µL of H_2O_2 and 14 µL of targets were mixed in ice bag and applied on sample pad. Color change was observed in the bulky of SiNPs on LFA platform.

2.2.5. Quantification of Color on LFA

ImageJ software (Caroline A Schneider, Wayne S Rasband and Kevin W Eliceiri, 2012) was used for analysis of images, which are taken on Stereomicroscope (1X) (Nikon, SMZ800). By adjusting color threshold with black background, blue color was signed. The image was transformed into 8 bite a grayscale image. Image was analyzed via lanes by plotting graph. Graph was gives Signal Intensity below formula.

$$SI = \log_{10}(255/\text{pixel value})$$

2.2.6. Statistical Analysis

GraphPad 7 was used for statistical analysis of SI: mean, standard error of mean and ANOVA. One-way ANOVA at 95% Confidence Interval and 99% Confidence Interval and Tukey test were applied on all data.

2.2.7. Optimization of Nucleic Acid Coated Nanoparticle Based LFA

2.2.7.1. H_2O_2 Concentration

Null SiNPs were prepared by following the preparation of SiNPs method and LFA test strips were constructed by folowing the preparation of LFA platform. 26 µL of H_2O_2 and 14 µL of MilliQ were mixed and applied on sample pad. Concentrations of H_2O_2 were varied as 1%, 1.5%, 2.5% and 3.5% (w/v). Images were captured with by Nikon, SMZ800 camera and analyzed by applying previous quantification and statistical analysis methods.

2.2.7.2. TMB concentration

Different TMB concentrations (2mM, 5mM and 10mM) were loaded on SiNPs by following the preparation of SiNPs method. SiNPs were capped with Probe-1. To check background signals and specificity at the same time, as a sample, complementary 284 bp target amplicon of *InvA* (*Salmonella* specific gene), 292 bp control amplicon of *ycdT* (*E. coli* specific gene) and only H_2O_2 were separately applied on LFA after getting single stranded amplicons. Photographs were taken by Nikon, SMZ800 camera and analyzed above quantification and statistical analysis methods.

2.2.7.3. HRP Concentration

One of colorimetric reaction components is horseradish peroxidase (HRP) (Sigma-Aldrich). HRP with concentration of 0.5 mg/mL and 1 mg/mL (≥250

units/mg) were located on nitrocellulose membrane. SiNPs were prepared by following preparation of SiNPs method as previously described. Target amplicon, control amplicon and only H_2O_2 run on separate LFAs. Images were recorded and analyzed.

2.2.7.4. Temperature

37 ^oC and room temperature were selected for all incubation steps (TMB entrapping, surface functionalization of APS, capping with probes) in the functionalization of SiNPs. Target amplicon, control amplicon and only H_2O_2 were separately applied on LFA and analyzed by ImageJ.

2.2.7.5. Duration of Silanization

During silanization, APS was introduced to SiNPs for various durations such as 1.5 hours and 3 hours. Probes were allowed to cap SiNPs by following capping procedure. Tests on LFAs were carried out with target amplicon, control amplicon and only H_2O_2 separately. Images of LFAs were analyzed by ImageJ and GraphPad.

2.2.7.6. Oligonucleotide Probe Concentrations

Oligonucleotide Probes with concentration of 100 μM and 200 μM were used for capping silanized SiNPs. Functionalized SiNPs were incubated with probes and located on LFA platform. Target amplicon, control amplicon and only H_2O_2 were separately applied on LFA platform. Their images were analyzed with ImageJ and GraphPad.

2.2.7.7. Flow Rate of Nitrocellulose Membrane

Nitrocellulose membranes with different flow rates were tried on this study. HRP and functionalized SiNPs were placed on HF180 and HF240 nitrocellulose

membrane. Target amplicon, control amplicon and only H_2O_2 were sent to LFAs. The intensity of blue color was measured with ImageJ and analyzed via GraphPad.

2.2.7.8. Position of HRP on Nitrocellulose Membrane

The position of SiNPs was fixed on nitrocellulose membrane and by changing HRP position and location, color change and specifity was checked. HRP were placed 3 mm above, 2 mm below and 3 mm below SiNPs

2.2.8. Specificity of the Assay

2.2.8.1. Colorimetric Response of Complementary Oligonucleotide Capped SiNPs

To check specificity of SiNPs based LFAs, two complementary oligonucleotide probes (Probe-1 and Probe-2) and uncomplementary probe were used. Additionally, to check the colorimetric reaction, Null SiNPs were obtained by adding MilliQ instead of probe. Probe-1 and Probe-2 were complementary to the 5' end of target amplicon and middle of target amplicon, respectively. It was investigated how the binding position of probes affected signal intensities. As a sample, target amplicon, control amplicon and only H_2O_2 were applied on LFAs for each of the probe capped and Null SiNPs. The organization of strip and samples were demonstrated in Figure 2.2. Results, SI values, were recorded and statistically analyzed with ImageJ and GraphPad.

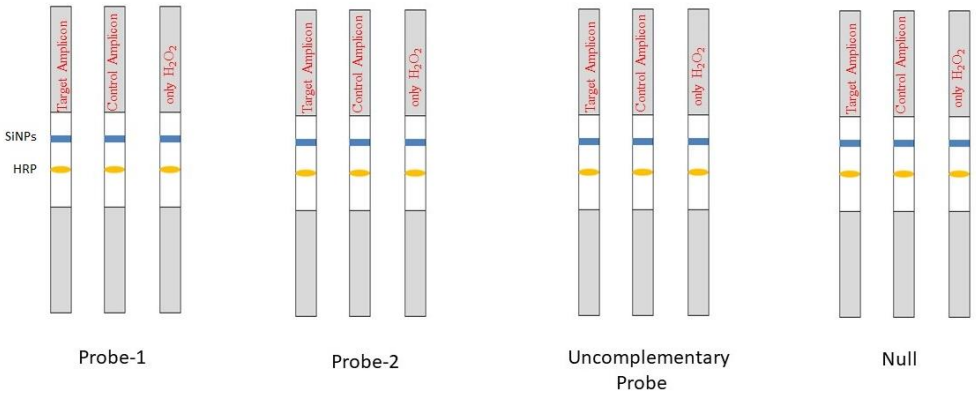

Figure 2.2: Experimental scheme of colorimetric response of complementary oligonucleotide (Probe-1 and Probe-2) capped SiNPs, Uncomplimentary Probe capped SiNPs and Null SiNPs on LFAs

2.2.8.2. Colorimetric Response of Complementary Oligonucleotide with Mismatches Capped SiNPs

To check specificity at the level of mismatch nucleotides, Mismatch Probe-1 and Mismatch Probe-2 were designed. They just differ from Probe-1 and Probe-2 with 3 mismatch nucleotides in the middle of probe. Probe-1 and Mismatch Probe-1, Probe-2 and Mismatch Probe-2 were compared by sending target amplicon, control amplicon and only H_2O_2. The organization of strip and samples were demonstrated in Figure 2.3. Their results on images were gathered and statistically analyzed.

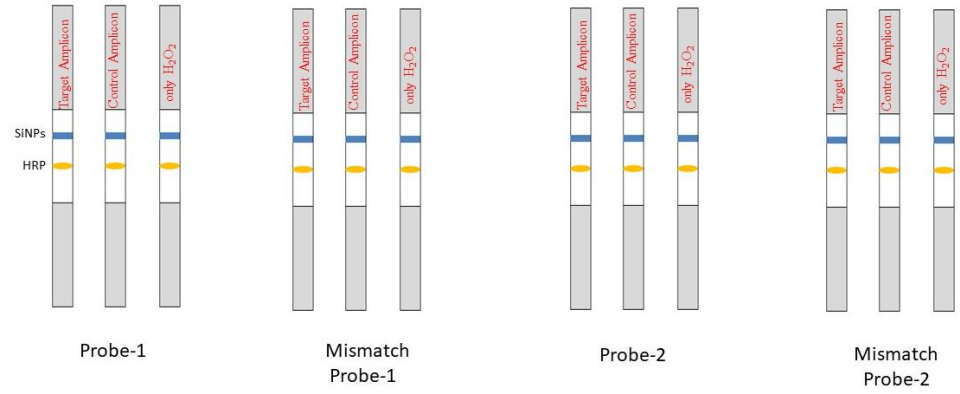

Figure 2.3: Experimental organization of colorimetric response of complementary oligonucleotide with mismatches capped SiNPs.

2.2.9. Sensitivity of the Assay

Another important criteria was sensitivity. To check its sensitivity, concentration of synthetic targets and different number of PCR cycles were compared in this study.

2.2.9.1. Limit of Detection for Synthetic Targets

Limit of detection (LoD) represents sensitivity of the assay. To check LoD, SiNPs, capped by Probe-1 and Probe-2, were prepared and placed on LFA platform. Target-1 and Target-2 are complementary to Probe-1 and Probe-2, respectively. Additionally, uncomplementary target sequence was employed as a control target. Each of complementary target was stocked at 100 μM. As a working solution, 10 μM, 1 μM and 0.5 μM of Target-1, Target-2 were prepared. Final concentration of target in 40 μL of sample mixture (26 μL of %1 H_2O_2 and 14 μL of targets) was arranged as 1000nM, 750 nM, 500nM, 250 nM, 100 nM, 75 nM, 25 nM, 10 nM, 5 nM and 0 nM. Final concentration of control in 40 μL of sample mixture was adjusted. Target-1, Target-2 and Control were applied on LFA. Their images were recorded and analyzed with ImageJ and GraphPad.

2.2.9.2. Limit of Detection for Amplicon

During optimization, amplicon was used. Thus, experiments with different numbers of PCR cycles were conducted to find out how many cycle is enough for detection. 40, 35, 30, 25, 20, 15, 10, 5 and 0 cycles were set on PCR for target amplicon. As control, control target was amplified with 40 cycle PCR. Each of them was separately applied on LFA. Their signal intensities were measured with ImageJ and analyzed withGraphPad.

CHAPTER 3

RESULTS AND DISCUSSION

3.1. General Experimental Principle

In the presence of hydrogen peroxide (H_2O_2), horseradish peroxidase (HRP) catalyzes 3,3′,5,5′-Tetramethylbenzidine (TMB) oxidation via redox reaction. TMB was entrapped in mesoporous (MSP) silica nanoparticles (SiNPs) while HRP was placed on nitrocellulose membrane and H_2O_2 was sent with samples. SiNPs have 2.1-2.7 nm narrow pore size. Concerning molecular size, TMB of 0.240 kD (Sigma-Aldrich, 2017) is smaller than HRP of 33.890 kD (Sigma-Aldrich, Peroxidase Enzymes, 2017). Thus, TMB can be entrapped into the SiNPs. TMB loaded SiNPs were functionalized with 3-aminopropyl trimethoxysilane (APS). APS chemically binds to the surface of SiNPs. Amino group on APS makes the surface positively charged. Positively charged surface can construct the ionic interaction with negatively charged phosphate backbone of oligonucleotide probes (E. Climent et al., 2010). Due to this ionic interaction, pores of SiNPs are closed by oligonucleotide probes. Similarly, oligonucleotides, aptamers and proteins are employed for capping nanoparticles in literature. These structures are called as molecular valve or nanovalves, which can be opened in the presence of external stimuli such as pH, temperature, specific DNA, protein or antibody (V. C. Ozalp and T. Schafer, 2011). In our study, complementary sequences make pores open by removing probe from the surface of SiNPs. By this way, TMB is released and oxidized in the presence of HRP and H_2O_2. On the other hand, the lack of a complementary sequence keeps pores close and TMB can be withhold inside SiNPs (Akça, 2014).

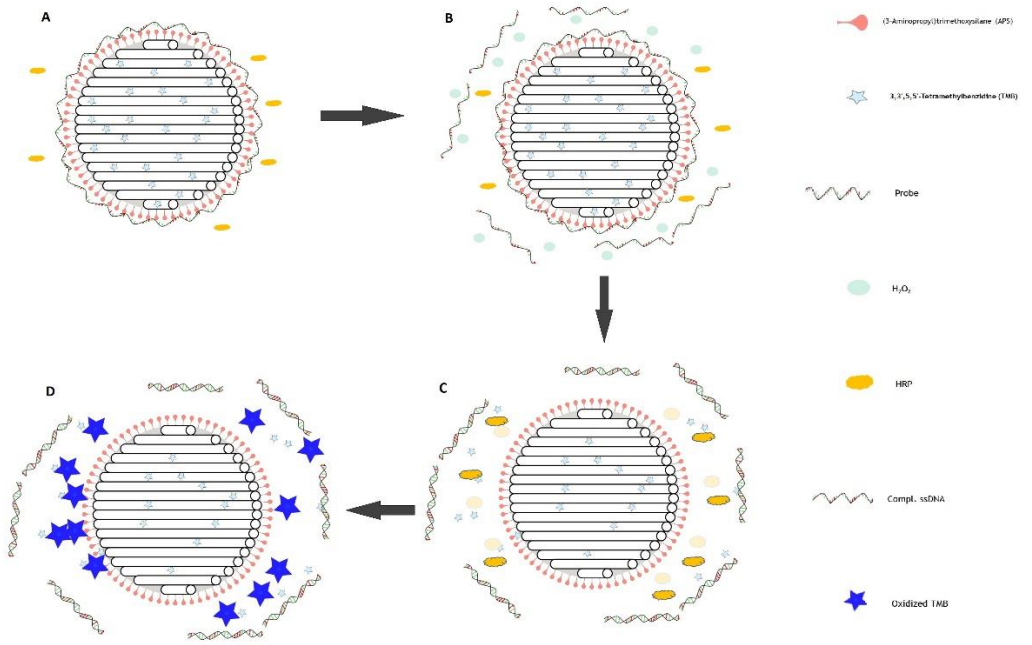

Figure 3.1: Schematic representation of working principle of TMB entrapped and Capped SiNPs**.** A) To close pores, SiNPs are silanized and oligonucleotide probes can ionically interact with silanized surface. By this way, TMB is entrapped in SiNPs via capping. Moreover, HRP is located outside SiNPs on nitrocellulose membrane. B) The sample including DNA and H_2O_2 is applied together. C) Complementary target hybridizes with oligonucleotide probes and make probes away from pores so that TMB can be released. D) In the presence of H_2O_2-HRP, released TMB is oxidized and the reaction can be simultaneously visualized with blue color. (Figure is inspired from (Akça, 2014)

3.2. Optimization Studies

To optimize the system, optimization experiments were carried out SiNPs on LFA platform since the components of LFA platform effects on reaction rate and reaction kinetics (H. V. Hsieh, J. L. Dantzler and B. H. Weigl, 2017). For this purpose, components of TMB-H_2O_2-HRP system, materials in functionalization of SiNPs and kinds of nitrocellulose membrane were studied.

3.2.1. Optimization of Colorimetric Reaction Parameters

TMB-H_2O_2-HRP reaction with colorimetric outcome is a kind of redox mechanism. TMB has aromatic amine which can be oxidized by HRP with H_2O_2. During first electron transfer, intermediates such as cationic free radical and charge transfer complex are generated. Charge transfer complex seems blue with

the absorbance peaks at 370 nm and 652 nm. Further oxidation of TMB was seen in the removal of second electron and diimine was produced at the end of all reaction. Diimine appears in yellow at 450 nm (Figure 3.2). The presence of H^+ ions enhances the diimine propagation (P. D. Josephy, et al, 1982). Thus, as a stop solution, H_2SO_4 is commonly used in this colorimetric reaction. However, Acidic condition damages amino group of APS. pK_a values of APS was defined at around 9.7 and 6.7 (Mathieu Etienne, Alain Walcarius, 2003). Under acidic conditions, silanized surface cannot preserve strong positively charged surface and unspecific TMB release and oxidation could be observed. Thus, the stop solution was not employed in our system. Also, it was aimed that the colorimetric reaction was kept in equilibrium with blue color for naked eye visualization. For this purpose, different concentrations of TMB, H_2O_2 and HRP were evaluated in this study.

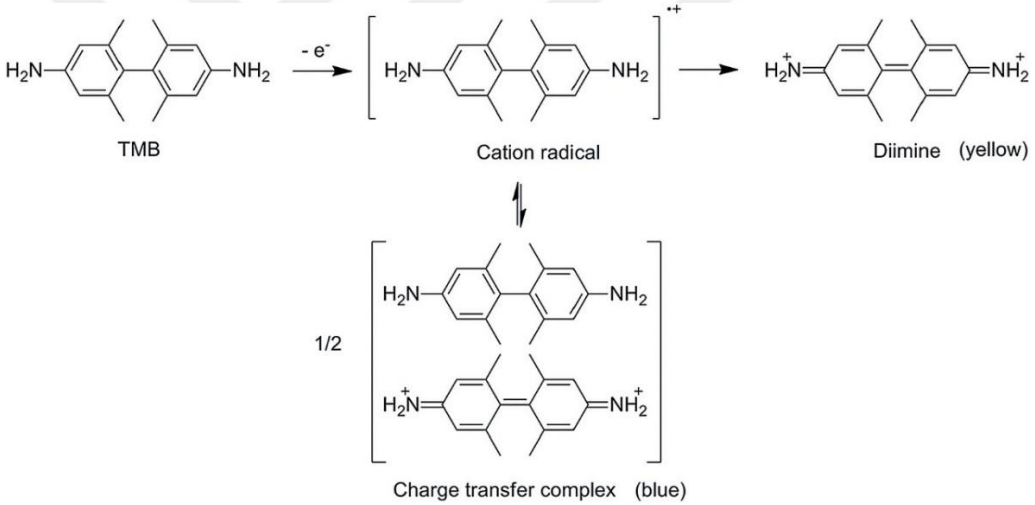

Figure 3.2: Schematic representation of two-step TMB conversion reaction (P. D. Josephy et al. 1982).

3.2.1.1. Effect of Different Concentrations of Hydrogen Peroxide

In the system of TMB-H_2O_2-HRP, H_2O_2 is oxidizing agent and thus accepts electrons coming from TMB. Peroxidase activity of HRP generates H_2O from H_2O_2. Additionally, the reaction rate and kinetics also depended on properties of LFA platform so all optimization experiments were carried out on LFA platforms. Thus, preliminary experiments were performed with null SiNPs, loaded with 2

mM of TMB. Only H_2O_2 with concentrations of 1%, 1.5%, 2.5% and 3.5% (w/v) were applied on LFAs.

In this colorimetric reaction, there is a ping pong mechanism. At the beginning of reaction, HRP reacts with H_2O_2 and they form HRP-oxygen free radical. Enzyme-oxygen free radical will be able to oxidize TMB. The concentration of H_2O_2 affects the formation of enzyme-oxygen free radicals so initial reaction rate will be affected (Gao L, Wu J and Gao D., 2011), (Josefa Hernander- Ruiz, Marino B. Arnao, Alexander N. P. Hiner, Francisco Garci, 2001). Different concentrations of H_2O_2 were tested to observe blue color formation on LFA. Blue color was quantified via grayscale image, generated in ImageJ analyzer software. H_2O_2 with 1%, 1.5%, 2.5% and 3.5%(w/v) was tested in optimization experiments (Figure 3.3). However, remarkable difference was not found, according to one-way ANOVA ($P>0.05$, $n=3$). It was observed that the 1% H_2O_2 produced the highest amount of SI on LFA platforms. Thus, we preferred 1% H_2O_2 for further studies. At high concentration of H_2O_2, HRP activity was inhibited even if there is no linear inhibition on signal intensities. However, the inhibition can be restricted at higher concentration of H_2O_2 by using magnetic nanoparticles (L. Gao, J. Zhuang, L. Nie and J. Zhang, 2007).

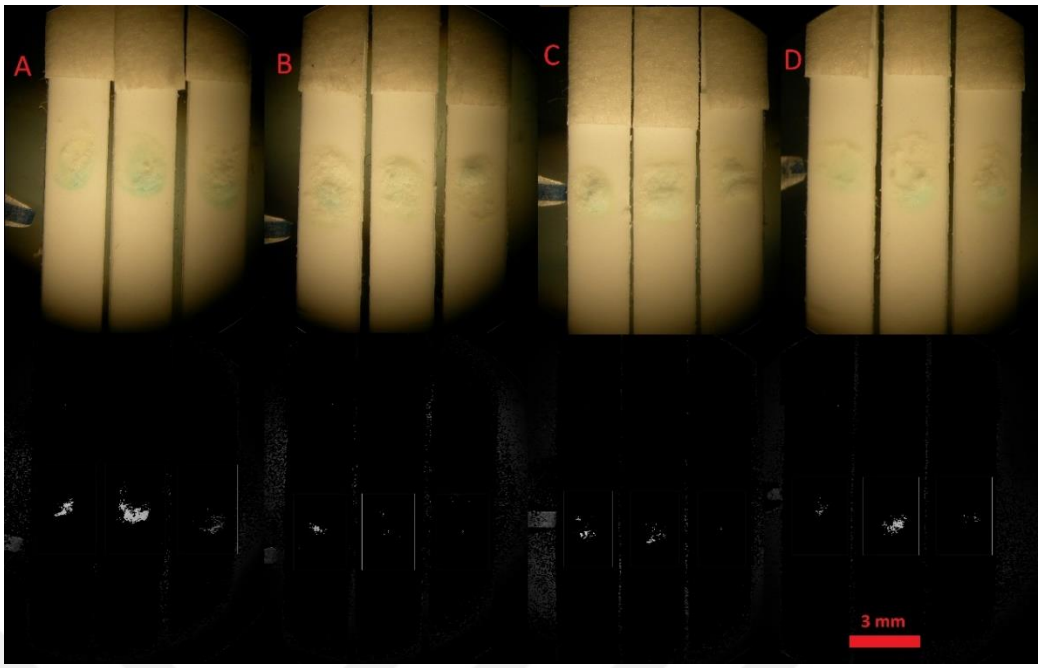

Figure 3.3: Various concentrations of H_2O_2 were applied on LFA platforms. ([TMB]=2 mM, 1 mg/mL HRP, room temperature) All SiNPs were prepared with 2mM of TMB and were silanized but oligonucleotide probes were not used for capping SiNPs. Null SiNPs were placed on LFA platforms. Their signal intensities (SI) were measured via ImageJ analyzes. ImageJ transform the image into grayscale image which was seen below. A) 1%(w/v) H_2O_2 was sent. B) 1.5% H_2O_2 was applied. C) 2.5% H_2O_2 was added onto LFA platforms. D) 3.5% H_2O_2 was applied.

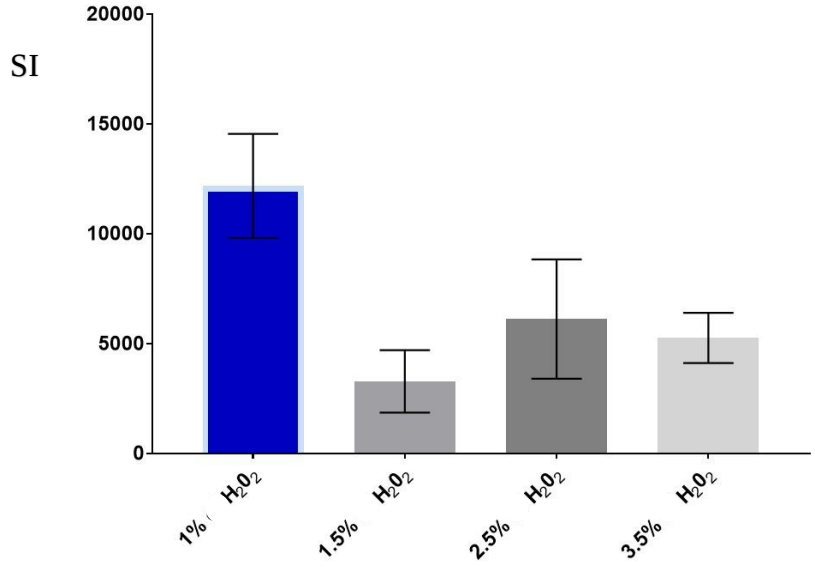

Figure 3.4: Signal Intensities (SIs) for various concentration of H_2O_2: 1%, 1.5%, 2.5% and 3.5% H_2O_2. Even though there is not any meaningful difference between concentrations of H_2O_2 (ANOVA, $P>0.05$); 1% H_2O_2, blue in graph, gives highest SI.

3.2.1.2. Effect of Different Concentrations of 3,3′,5,5′-Tetramethylbenzidine (TMB)

TMB is the reducing part of the colorimetric reaction. Blue color was observed when TMB was oxidized via donating an electron into the system. Charge transfer complex was obtained in rapid equilibrium due to oxidation (P. David Josephy et al., 1982). Preferred outcome parameter of the assay's platform to get higher signal intensity with specificity is critical in this study. Thus, different concentrations (2mM, 5mM and 10mM) of TMB were tested. SiNPs, capped with Probe-1 which were composed of complementary sequence to *InvA* gene, were placed on LFAs. As samples, target including complementary 284 bp amplicon of *InvA* gene and H_2O_2, control consisting of 292 bp uncomplementary amplicon and only H_2O_2 without amplicon were applied on LFAs. 2mM of TMB loaded SiNPs could not discriminate target sequence and controls (one-way ANOVA, $P>0.05$, $n=3$). Additionally, it produced low amount of SI on LFAs and the color formation seem very low. 5mM of TMB loaded SiNPs could generate true color on strips and generated higher SI on target sent strips than controls (one-way ANOVA and Tukey HSD test, $P<0.001$). 10mM of TMB loaded SiNPs also produced high amount of SI but its specificity was not as good as 5mM. High amount of SI was also seen on controls. However, there was insignificant differences between target, control and and H_2O_2. Thus, specificity was not meaningful in 10mM of TMB loaded SiNPs (one-way ANOVA, $P>0.05$). During silanization and probe capping, SiNPs were incubated in aqueous environment. At high concentration, TMB molecules could have clung on, the surface of SiNPs, APS molecules or probes. Thus, even though pores are closed during colorimetric reaction, TMB, clung on APS and probes, could generate blue color. Moreover, the oxidation of TMB releases H^+ ions which damage ionic interaction of probes and silanized surface. Thus, high concentration of TMB could also cause the leakage of TMB. TMB concentration of 5mM was chosen in further experiments.

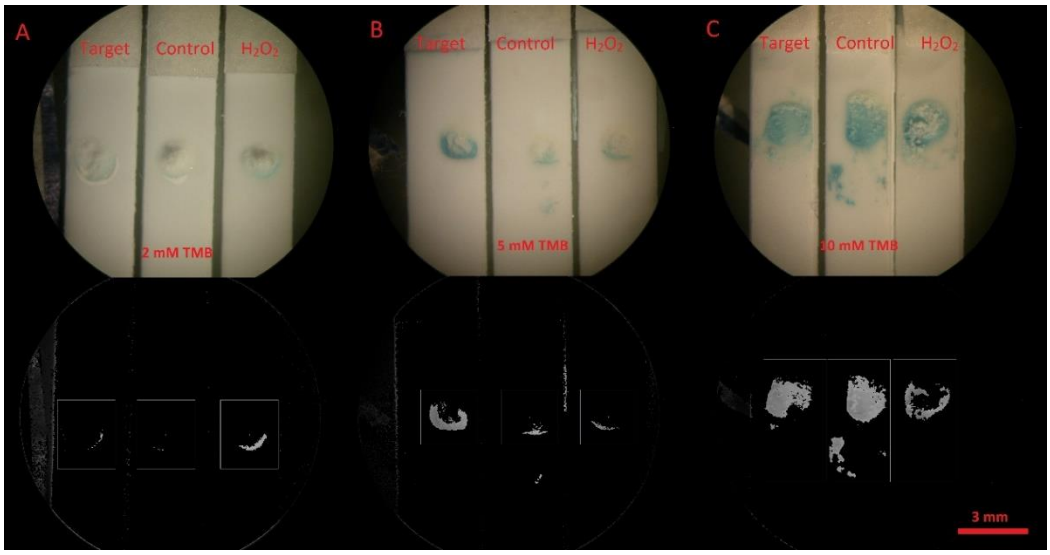

Figure 3.5: Colorimetric reactions on LFA with different concentration of TMB. SiNPs were loaded with 2mM, 5mM and 10 mM of TMB. Pores on SiNPs were capped with Probe-1 and located on LFA platforms. (1% H_2O_2, 1 mg/mL of HRP and room temperature) Target (including complementary sequence), Control (composed of uncomplimentary sequence) were applied with 1% H_2O_2 to LFAs. Without nucleic acids, only 1% H_2O_2 was also applied as second control. A) SiNPs onto which 2mM of TMB was loaded B) SiNPs with 5mM of TMB C) 10 mM of TMB loaded SiNPs

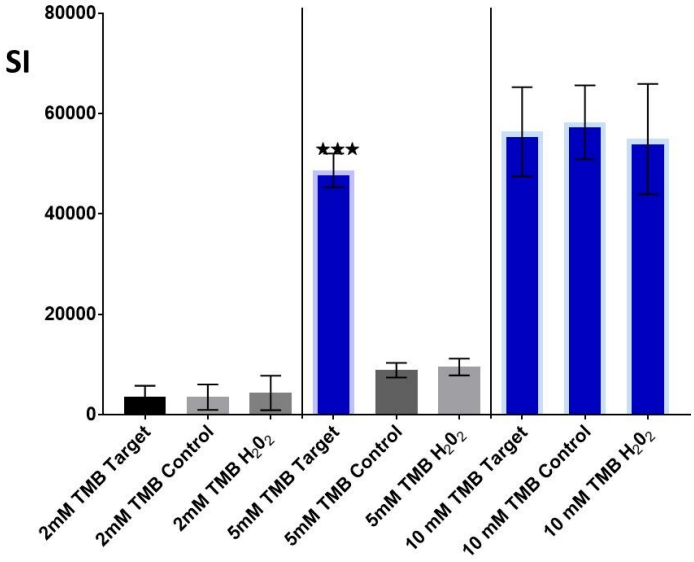

Figure 3.6: Signal Intensity (SI) for various TMB concentration 2mM, 5 mM and 10mM) on LFA with Probe-1 capped SiNPs. there was not significant SI on 2mM and 10 mM of TMB (one-way ANOVA, $P>0.05$, n=3) while LFAs, on which target was applied, significantly differentiated from control and H_2O_2 (one-way ANOVA, Tukey HSD test, $P>0.05$, n=3).

3.2.1.3. Effect of Different Concentrations of Horseradish Peroxidase (HRP)

The last component of the colorimetric reaction is HRP, which is the catalytic enzyme of reaction. Initially, HRP reacts with oxygen and form an enzyme-oxygen free radical. The enzyme-oxygen free radical reacts with TMB (Gao L et al., 2011). Two concentrations of HRP (0.5 mg/mL and 1 mg/mL) were used in optimization experiments. Respectively, 0.5 mg/mL and 1 mg/mL of HRP were totally placed on nitrocellulose membrane. Their SI and sensitivity were almost same. Both on concentrations gave significantly selective signals (one-way ANOVA, Tukey HSD test, $P<0.001$, $n=3$). 0.5mg/mL of HRP created slightly less amount of SIs than 1 mg/mL of HRP, which was not statistically meaningful. On the other hand, 0.5 mg/mL of HRP could discriminate slightly better than 1 mg/mL of HRP. 0.5 mg/mL of HRP was used for further studies because of higher specificity and the decrease in the cost of the assay.

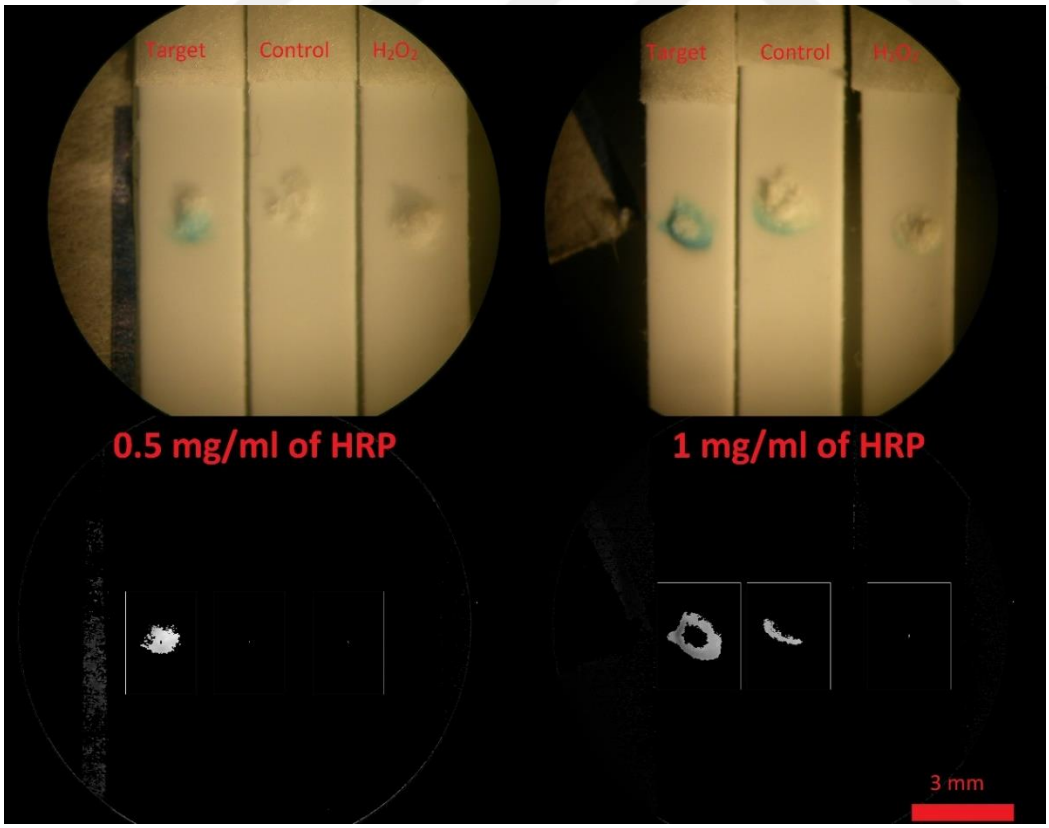

Figure 3.7: The response of LFAs for 0.5 mg/mL and 1 mg/mL of HRP ([TMB] = 5 mM, 1% H_2O_2, and room temperature)

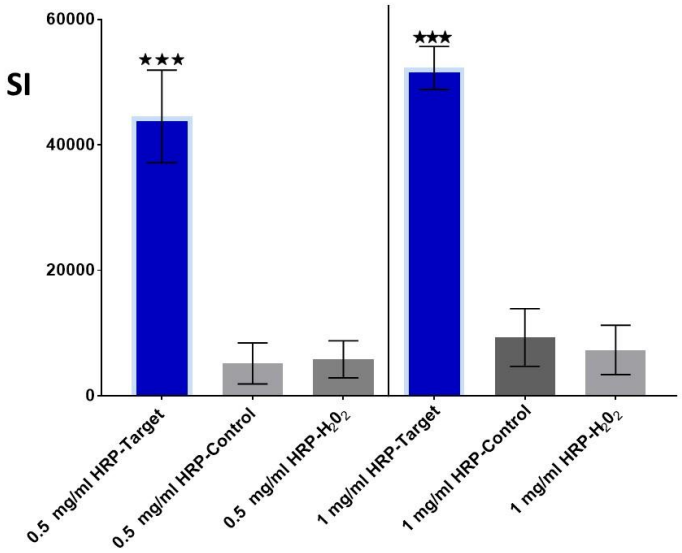

Figure 3.8: SI of 0.5 mg/mL of HRP and 1 mg/mL of HRP. Into both concentration, SiNPs were capped with Probe-1. Target, control and only H_2O_2 were applied (one-way ANOVA, Tukey HSD test, $P<0.001$, n=3).

3.2.1.4. Effect of Different Temperatures of Silanization on Oligo-Capping

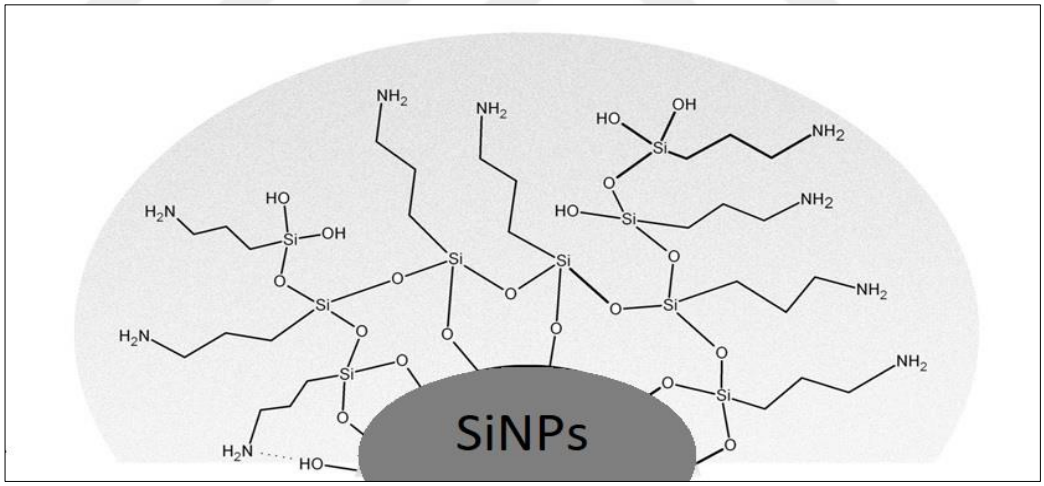

Figure 3.9: Representation of unproperly silanized surface of SiNPs (inspired from Rafael A. Bini, e*t al*., 2011).

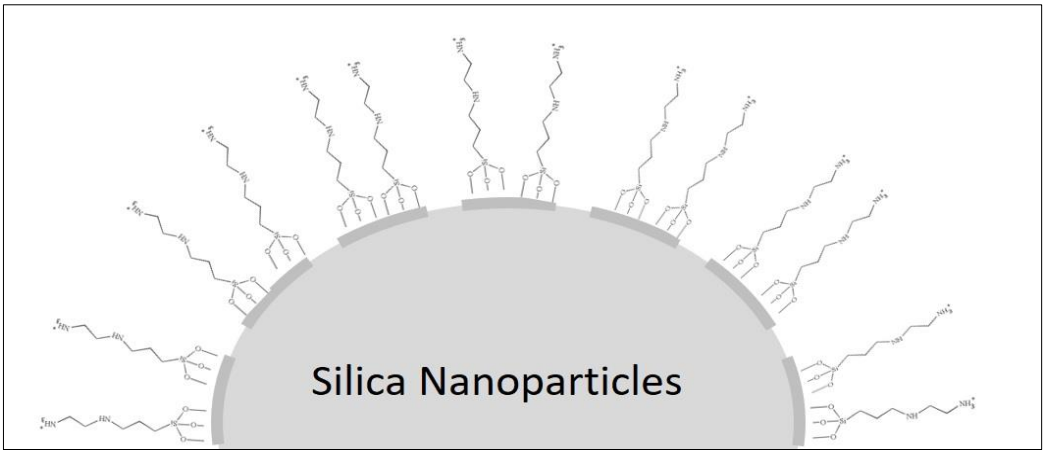

Figure 3.10: Representation of required silanization of SiNPs (inspired from Rafael A. Bini, e*t al*., 2011)

SiNPs are modified by APS so that their surface can be acceptable for probes. APS molecules chemically bind to the surface of SiNPs. Silane molecules can construct the bridge between SiNPs and oligonucleotides (Rafael A. Bini, at al., 2011). Moreover, to bind oligonucleotide probes, amino group must accommodate outer part of SiNPs, which can be provided by proper silanization procedure. The phosphate backbone of oligonucleotides is negatively charged. Positively charged silanized surface can construct ionic bounds with oligonucleotides. This situation was maintained with proper orientation of silanization which depends on temperature and pH (Figure 3.10). At pH 7.5, more amino groups on APS (pK= 6.7) are positively charged. Thus, PBS with 7.5 pH was used during silanization and probe capping procedures. Temperature is another affecting factor on silanization (Robert G. Acres et al., 2014). Change on temperature causes the conformational change on DNA and damages linearity of probes and their hybridization with target. For this purpose, we compared SI of SiNPs which were prepared at room temperature and 37^{o}C. it was showed that silanization at 37^{o}C created more specific (one-way ANOVA, Tukey HSD test, $P<0.001$, $n=3$) and high amount of SI comparing ones at room temperature. Due to lack of proper silanization at room temperature and also in steps following silanization, some amount of TMB would be leaked. Silane molecules might vary their own orientation on the surface of SiNPs (Figure 3.9). The amount of amino group on the surface of SiNPs might be diminished so that probe could not be properly cap pores. Thus, SI might be low and unspecific (one-way ANOVA,

P>0.05, n=3). However, at 37°C, it was found that more specific and high signal intensities. Further experiments were continued with silanization at 37°C.

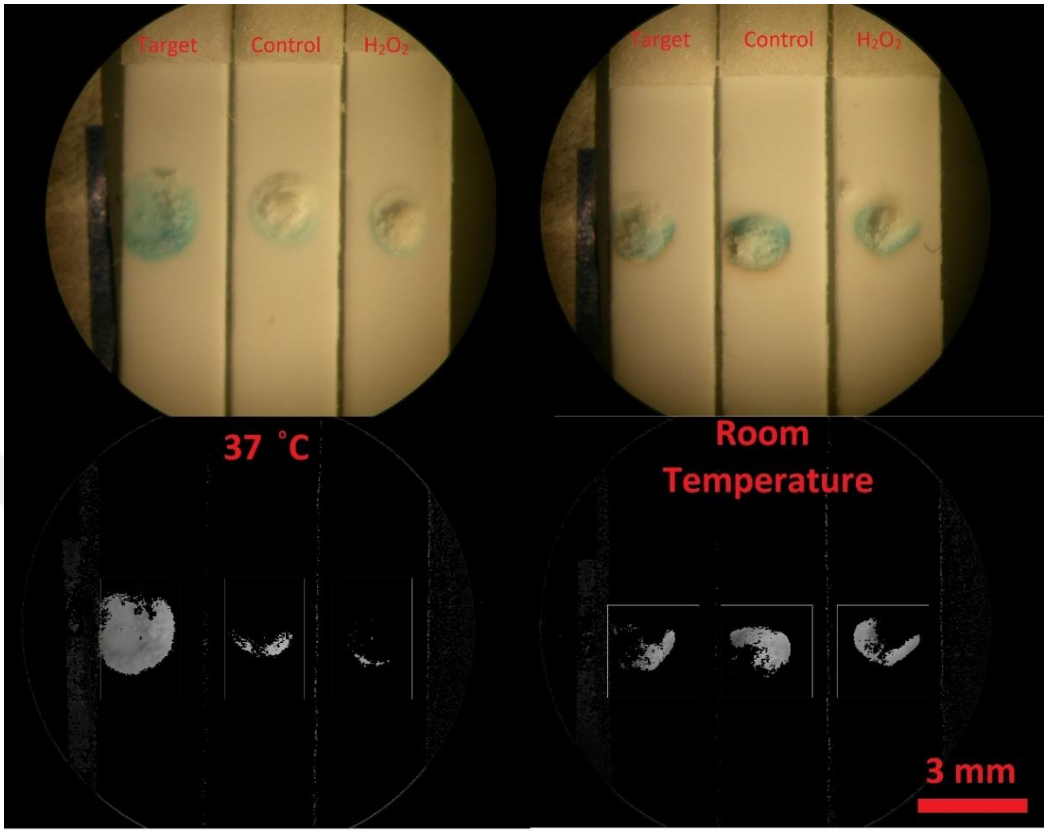

Figure 3.11: Photographs of SI on LFA in which SiNPs had been prepared at different temperatures: 37°C and room temperature. ([TMB] = 5 mM, 1% H_2O_2, 0.5 mg/mL of HRP)

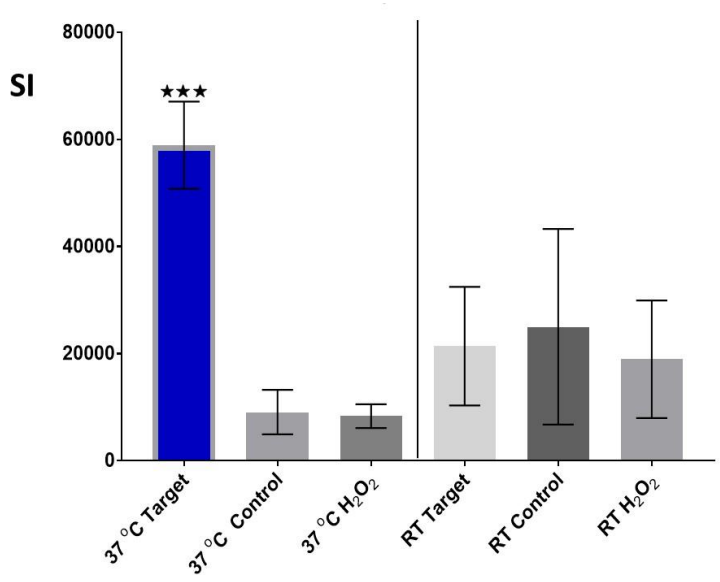

Figure 3.12: The graph of SI was obtained from SiNPs which had been prepared at 37ºC and room temperature. SIs of LFAs were meaningfully different among one at 37ºC (one-way ANOVA, Tukey HSD test, P<0.001, n=3) when there was not significant difference at room temperature (one-way ANOVA, P>0.05, n=3).

3.2.1.5. Effect of Different Duration of Silanization

Duration of silanization acts on proper functionalization of surface. Extended duration of APS creates multiple layer on surface. The formation of multiple layers varies orientations of APS on surface. Some amount of amino group on the surface was replaced with -CH_3 (John A. Howarter and Jeffrey P. Youngblood, 2006). Therefore, amino groups on the surface of SiNPs were not enough to interact with probes. In the previous experiments, silanization took 3 hours but background signals were always gathered from SiNPs based LFAs. The possible reason is the leakage or the residue of TMB on SiNPs. It was thought that some amount of TMB could have been squeezed in multiple layer of APS. Thus, it was aimed to prevent multiple layer formation on surface by decreasing in duration of silanization. Two different durations (1.5 hours and 3 hours) of silanization were checked in these experiments. 3 hours silanization made SiNPs based LFAs high response and high specificity (one-way ANOVA, Tukey HSD test, P<0.001, n=3). 1.5 hours incubation of APS could not generate specific response on LFAs (one-way ANOVA, P>0.05, n=3). The possible reason is the leakage of TMB. There must not have been enough positively charged amino groups and so ionic interaction between oligonucleotide probes and surface could not be constructed.

As a result of the lack of the ionic interaction, pores of SiNPs could not be capped. Therefore, in the following steps to silanization, TMB must have been lost so low signal intensities was recorded. Without concerning the presence of target, more amount of signal on LFAs was detected in 1.5 hours silanization than 3 hour silanized SiNPs. The leakage of TMB also caused to gather signals from controls. Thus, we maintained to perform experiments with 3 hours silanization procedure.

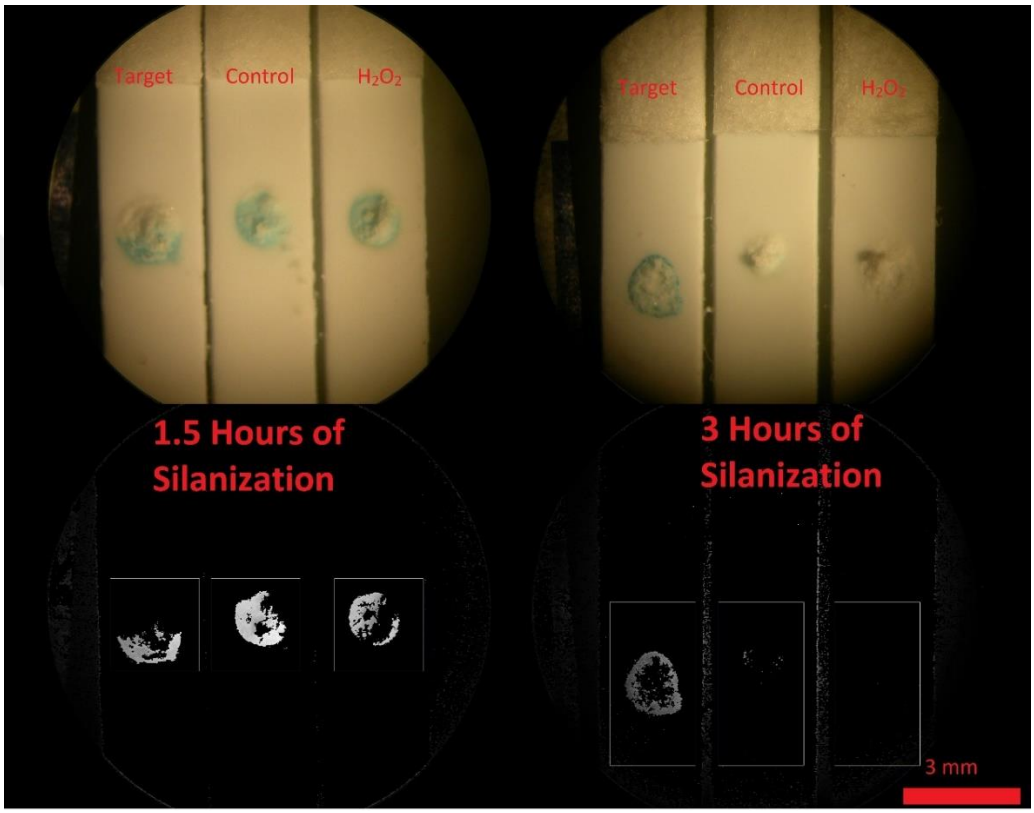

Figure 3.13: Images of LFA in which SiNPs were prepared with 1.5 hours and 3 hours silanization. ([TMB] = 5 mM, 1% H_2O_2, 0.5 mg/mL of HRP and 37ºC)

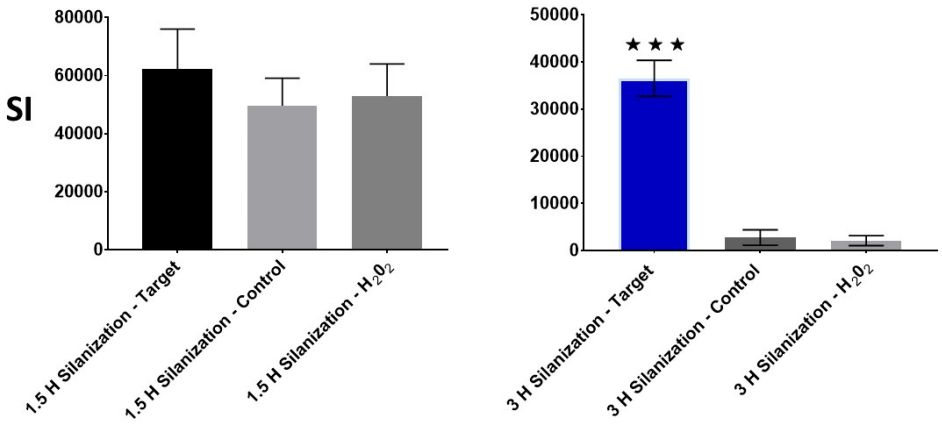

Figure 3.14: The graph of SI was obtained from SiNPs which had been prepared with 1.5 hours and 3 hours silanization. Target caused significantly high SI on LFAs, prepared with 3 hours silanization (one-way ANOVA, Tukey HSD test, $P<0.001$, $n=3$), while 1.5 hours silanization could not properly generate SI on LFAs (one-way ANOVA, $P>0.05$, $n=3$).

3.2.1.6. Concentration of Oligonucleotides

The other critical variable on functionalization of SiNPs is to cap pores with oligonucleotides. Our designed oligonucleotides probes were 34 bases long. The length of one single stranded base was observed as 0.7 nm while double stranded base was 0.34 nm (Jie Yan and John F. Marko, 2004). The length of oligonucleotides is theoretically calculated as 23.8 nm, which can easily cap multiple pores of SiNPs (2.1-2.4 nm diameter). Two different concentrations (100μM and 200 μM) of oligonucleotide probes were checked. Thus, there has not been any significant difference on SI between two probes' concentrations (one-way ANOVA, $P>0.05$, $n=3$). Both concentration of probes showed specific signal (one-way ANOVA, $P<0.001$). Owing to cost of HRP, 100μM was chosen as working parameter.

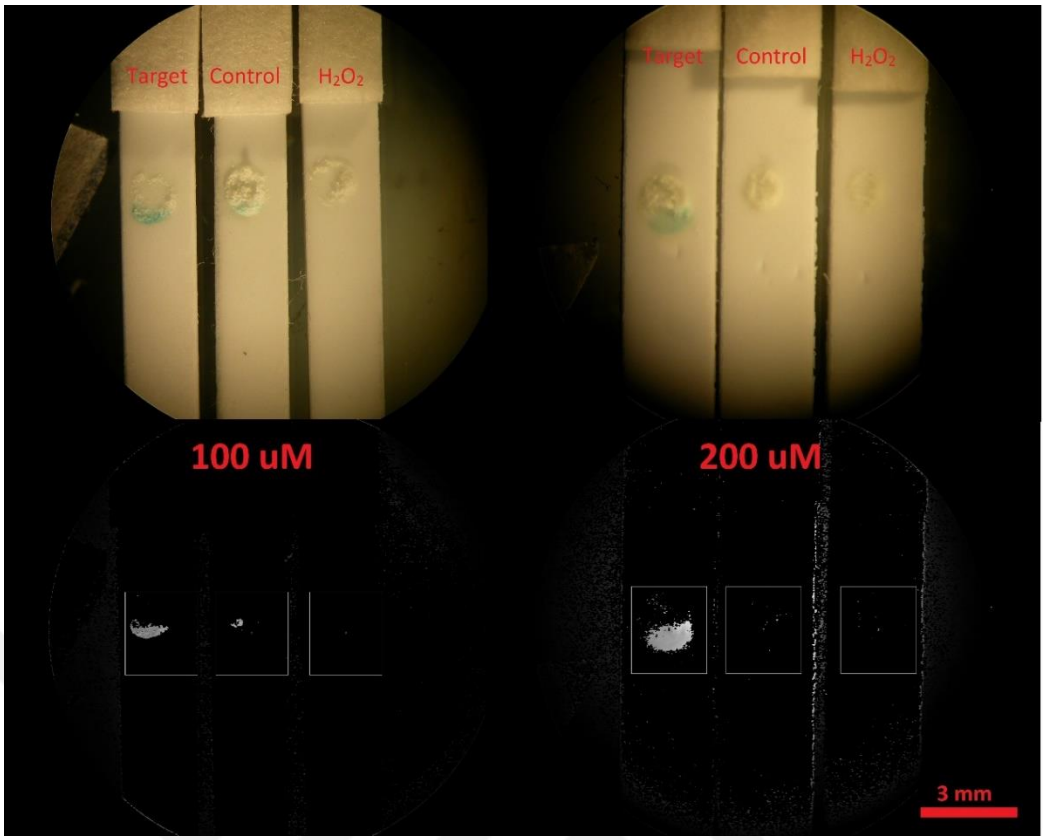

Figure 3.15: The images of LFA in which SiNPs were capped with 100uM and 200uM of oligonucleotide probes. ([TMB] = 5 mM, 1% H_2O_2, 0.5 mg/mL of HRP and 37°C)

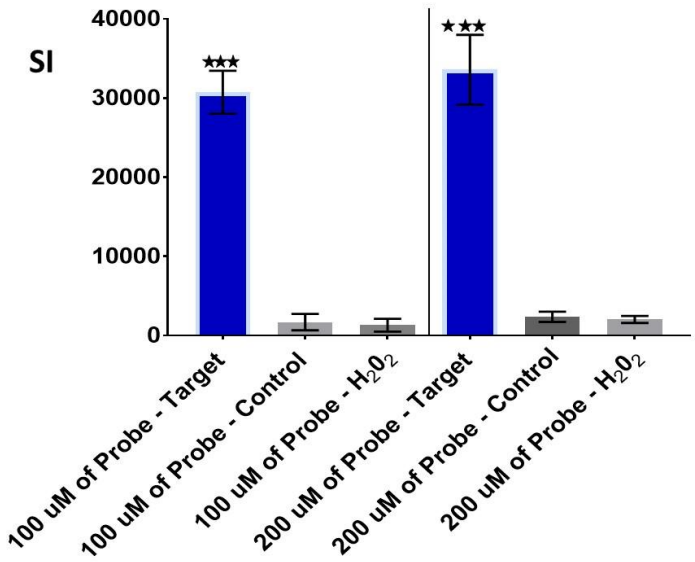

Figure 3.16: The graph of SI on LFAs in which SiNPs were prepared with 100uM and 200uM of oligonucleotide probes. Both concentrations of oligonucleotide probes significantly generate SI (one-way ANOVA, Tukey HSD test, $P<0.001$, n=3).

3.2.2. Optimization of Lateral Flow Assay Platform

In this study, LFA platform was constructed with three components: Sample pad, nitrocellulose membrane and absorbance pad. Sample pad and absorbent pad were same material, cellulosic fiber materials providing with porous matrices. Nitrocellulose membrane offers 10 times larger surface than other membrane due to the presence of internal porous structure. Nitrocellulose membrane is completely neutral and the ability of adsorption is independent on pH. In this study, we did not use conjugate pad. Conjugate pad brings sample or detector reagent onto membrane location (B. Ngom et.al, 2010). However, in this study, the colorimetric reaction of TMB-H_2O_2-HRP simultaneously occurred on nitrocellulose membrane and any secondary detection probe or antibody was not used and so reservoir part was not required in this study and flow was controlled by sample and absorbent pad at two ends of platform.

3.2.2.1. Flow Rate of Membrane

Nitrocelluose membranes are classified according to the flow rate. Flow rate of membrane was graded with sec/cm, which was coded as Hi-Flow (HF). In this study, HF180 (180 ± 45 sec/4cm) and HF240 (240 ± 45 sec/4cm) were compared. Slow flow rate, or high HF value enhances the sensitivity (B. Ngom et.al., 2010). Concerning SI on LFAs, there was not any significant difference and both have specific results (one-way ANOVA, Tukey HSD test, $P<0.001$, $n=3$). However, background signals or SI of controls was lower at HF240 than HF180. The flow rate at HF240 is slower than that of HF180. Thus, the probability of hybridization is higher at HF240 than one at HF180. Perfect hybridization enhances the specificity of LFA. Thus, background signals or SI of controls are lower at HF240. For further studies, HF240 nitrocellulose membrane were chosen to be used.

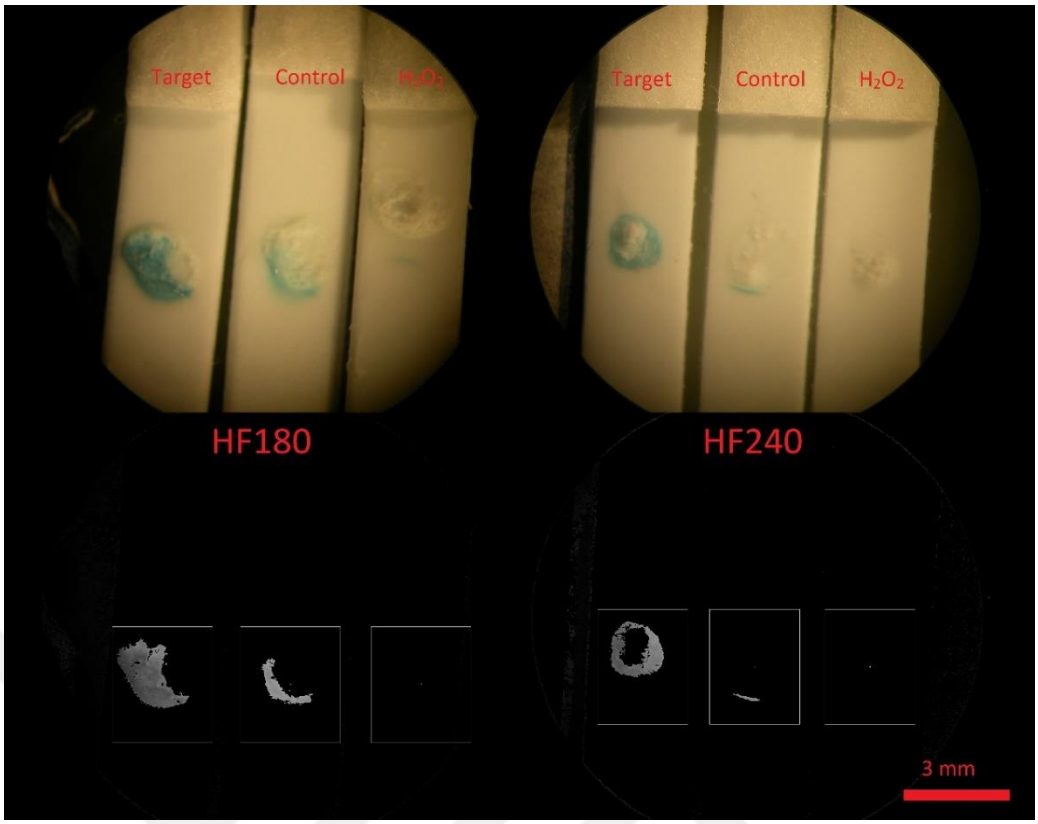

Figure 3.17: The images of LFAs with different nitrocellulose membranes: HF180 and HF240. ([TMB] = 5 mM, 1% H_2O_2, 0.5 mg/mL of HRP and 37°C)

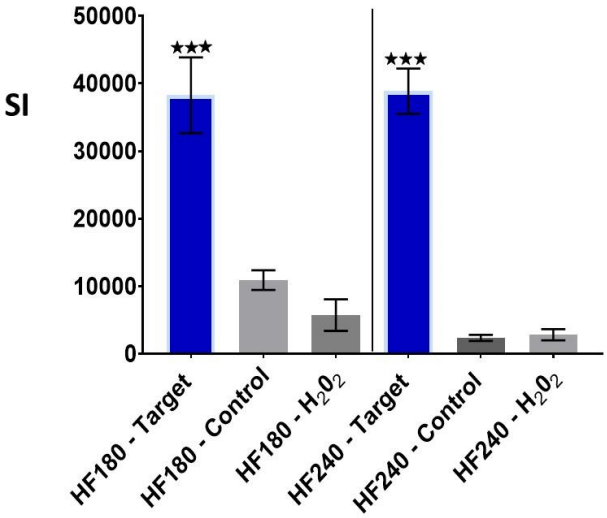

Figure 3.18: Graph of SI on LFAs with different flow rates: HF180 and HF240. Both flow rates could produce meaningfully specific response on LFAs (one-way ANOVA, Tukey HSD test, $P<0.001$, n=3)

3.2.2.2. Positions of Capped Nanoparticles and HRP

SiNPs were placed on 4 mm away from sample pad and the position of SiNPs on nitrocellulose membrane was fixed. The effect of positions of HRP was tested in this study. HRP was placed 3 mm above SiNPs, 2 mm below SiNPs and 3 mm below SiNPs. The LFA with HRP 3mm above SiNPs could not generate SI. Concerning flow rate, HRP was firstly meet with H_2O_2 and ssDNAs. HRP firstly interacts with H_2O_2 and get ready for oxidation. The aromatic structures of bases are prone to oxidation in the presence of HRP- H_2O_2 (Eleanor G. Rogan, Patricia A. Katomski, Robert W. Roth, and Ercole L. Cavalieri, 1979). The oxidation of bases obstructs hydrogen bonds in hybridization so the lack of hybridization could not open gates of SiNPs. On the other hand, HRP below SiNPs worked. After SiNPs were placed on nitrocellulose membrane, HRP was placed away from SiNPs. HRP diffused both direction and approached around SiNPs. Thus, colorimetric reaction occurred around SiNPs and color could be visualized on SiNPs. Both of HRPs, 2 mm and 3 mm below SiNPs could generate blue color. However, HRP 2 mm below SiNPs produced high and selective signal on LFAs (one-way ANOVA, Tukey HSD test, $P<0.001$, $n=3$). HRP was located 2mm below SiNPs.

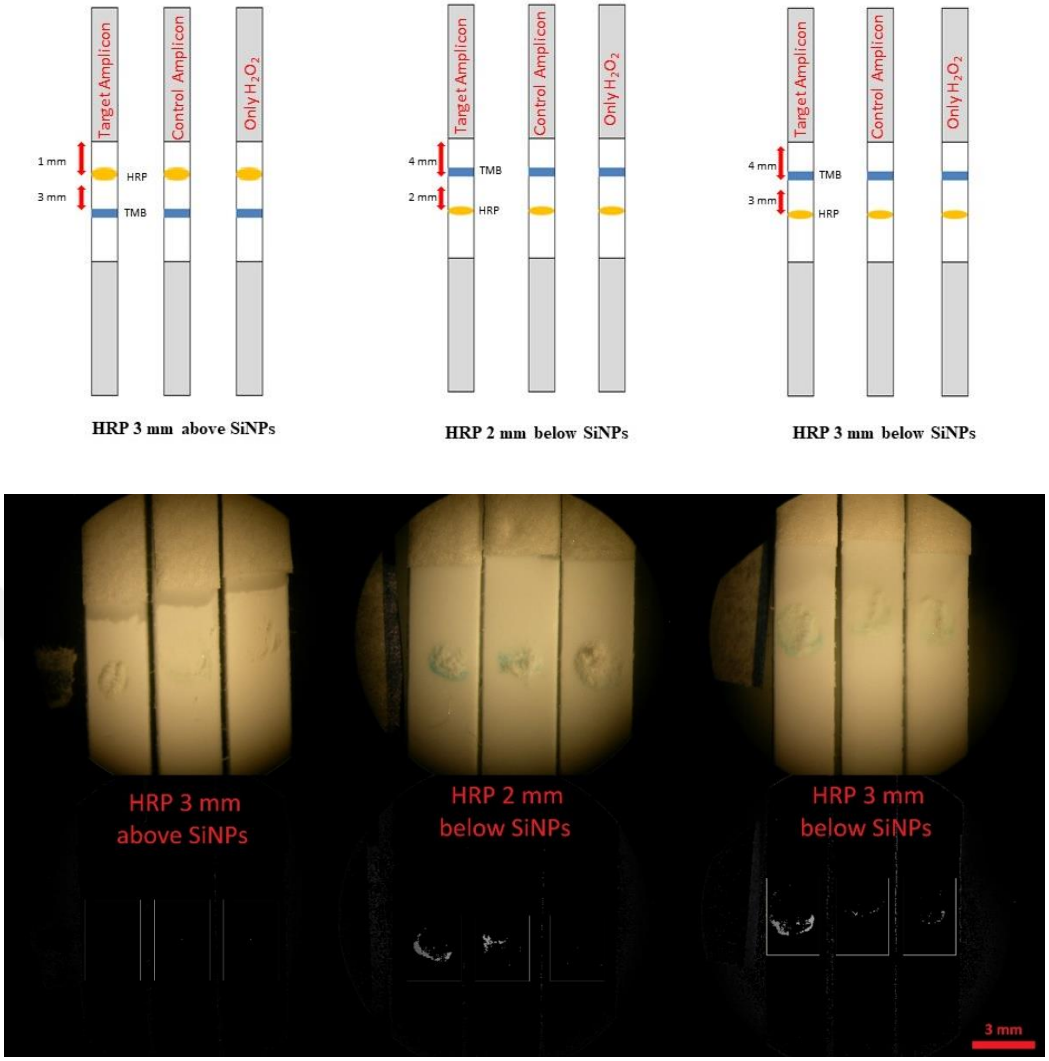

Figure 3.19: The image of LFAs in which HRPs were located on different positions: 3 mm above SiNPs, 2 mm below SiNPs and 3 mm below SiNPs. ([TMB] = 5 mM, 1% H_2O_2, 0.5 mg/mL of HRP and 37°C)

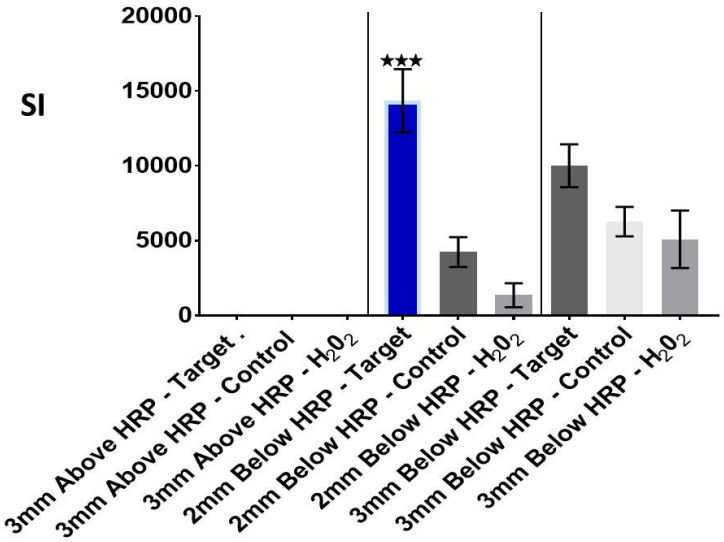

Figure 3.20: Signal intensity of LFA in which HRPs were posited on different locations: 3 mm above SiNPs, 2 mm below SiNPs and 3 mm below SiNPs. HRP 3 mm above SiNPs could not generate signal. HRP 2 mm below SiNPs significantly recognize target (one-way ANOVA, Tukey HSD test, $P<0.001$, n=3).

As a result of optimization experiments, 1% H_2O_2, 5 mM of TMB, 1 mg/mL of HRP, silanization at 37°C for 3 hours, 100 µM of oligonucleotide probes were chosen. In LFA platform, HF240 was used for following specificity and selectivity experiments.

3.3. Specificity of the Assay

The ability of an assay to identify one target substance was defined as specificity (Alfred J. Saah and Donald R. Hoover, 1997). To check the specificity of SiNP based LFA, we prepared SiNPs with complementary probes (Probe-1 and Probe-2) and uncomplementary probes. Additionally, for each probe, Target amplicon with complementary sequence to probes and control amplicon without complementary sequence were separately applied on LFAs. By using mismatched probes, the recognizing ability of SiNPs based LFA was evaluated. Specificity experiments was performed with all the previously optimized experimental parameters.

3.3.1. Colorimetric Response of Complementary DNA-Capped Silica

Figure 3. 21: Matching positions of complementary probes (Probe-1 and Probe-2) to target amplicon.

Probe-1 and Probe-2 were complementary to target amplicon on different positions. Probe-1 was complementary to the 5' end of target amplicon while Probe-2 was complementary to the middle of target amplicon. It was investigated how the binding position of probes affected to signal intensities. For each of probe, target amplicon, control amplicon and H_2O_2 were separately applied on LFAs. Probe-1 and Probe-2 sufficiently produced color signal to target amplicon while they do not give adequate response to control amplicon and H_2O_2 (ANOVA, Tukey HSD test, $p<0.001$, $n=15$). The meaningful difference between Probe-1 and Probe-2 was not found (one-way ANOVA, $P>0.05$, $n=15$). Thus, the complementary position of probe does not effect on signal generation on SiNPs based LFAs. The hybridization between probes and its own complementary sequence in target amplicon keeps probes away from SiNPs pores and TMB can be released from SiNPs. HRP around SiNPs forms enzyme-oxygen complex which oxidize TMB and the color of TMB is shifted to blue. On the other hand, control target and H_2O_2 do not have complementary sequence and so hybridization of probes cannot occur and TMB is still entrapped inside SiNPs. The change on color cannot be observed on LFAs. Similarly, uncomplementary probe does not have any complementary sequence to Target amplicon or control amplicon. Thus, we did not recognize any meaningful color change on LFAs.

Null SiNPs, prepared without probes on surface, were employed in this study. Null SiNPs were used for examination of colorimetric reaction independent of hybridization. Color was formed on all Null SiNPs, which shows that TMB-H_2O_2-HRP redox system properly worked on SiNPs based LFAs. However, The Signal Intensity of Null SiNPs was lower than probe capped SiNPs (ANOVA, Tukey

HSD test, $p<0.01$, $n=15$). During washing steps of SiNPs and capping steps may have caused to lose some amount of TMB. Thus, after oxidation, the signal must have been lower than probe capped SiNPs.

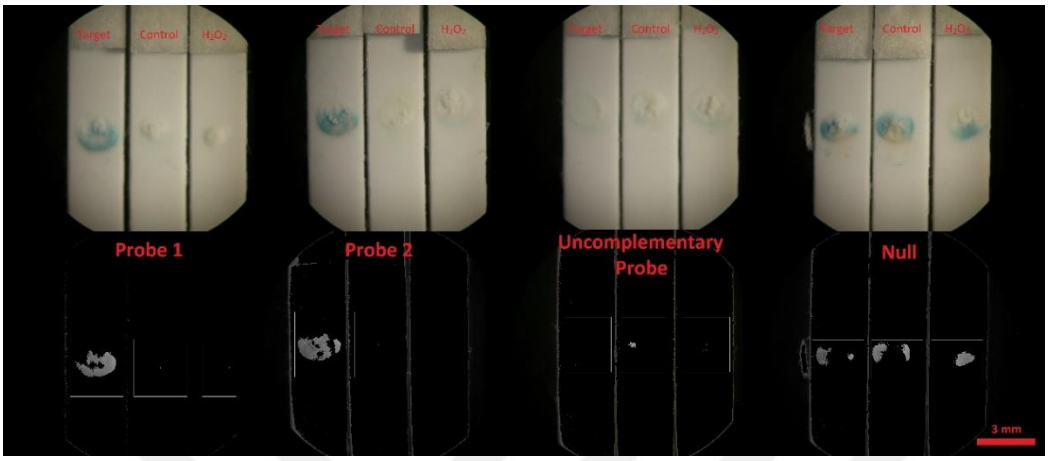

Figure 3.22: The image of LFAs including SiNPs capped with Probe-1, Probe-2, Uncomplementary Probe and uncapped. ([TMB] = 5 mM, 1% H2O2, 0.5 mg/mL of HRP and 37oC)

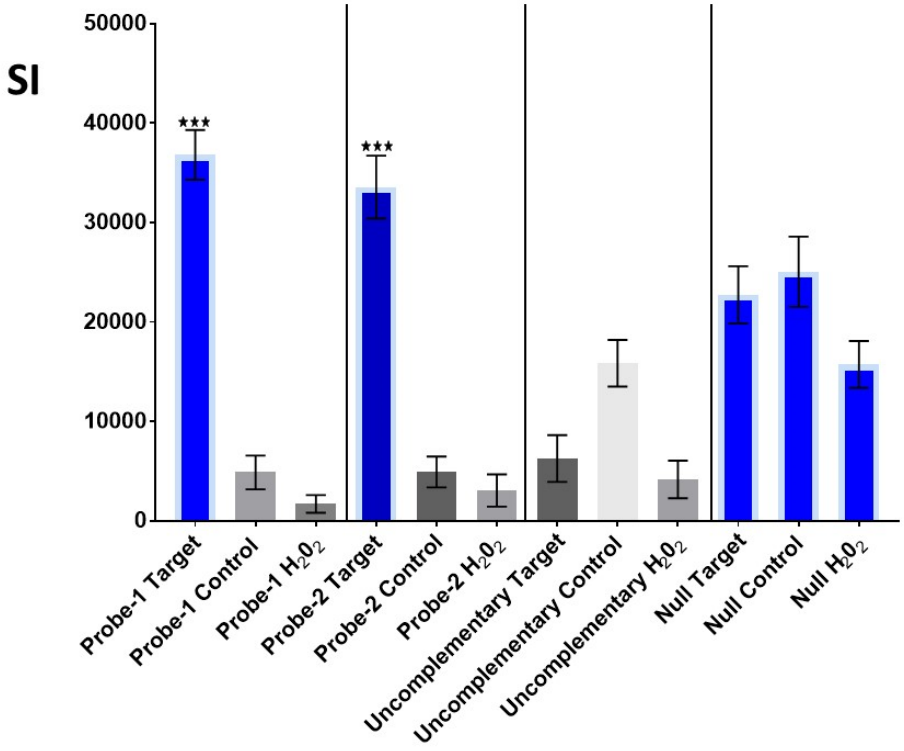

Figure 3.23: Signal intensity of LFA in which SiNPs were capped with Probe-1, Probe-2, Uncomplementary Probe and Null (uncapped). LFAs on which complementary targets were applied generated significantly high SI.

3.3.2. Colorimetric Response of Mismatched DNA-Capped Silica Nanoparticles

To check further specificity of SiNPs, mismatch probes were designed. Mismatch Probe-1 was derived with 3 mismatch bases from Probe-1 while Mismatch Probe-2 was derived with 3 mismatch bases from Probe-2. Mismatch probes could not generate sufficient signal to target amplicon while complementary probes could shift the color on blue with a sufficient amount of change. SiNPs capped with oligonucleotide probes could distinguish 3 mismatch bases on target amplicon (ANOVA, Tukey HSD test, $P<0.001$, $n=6$). These results indicated that 3 mismatches can be identified by SiNPs based LFAs. However, background signal was also measured on mismatch probes and control amplicon and H_2O_2. Some amount of TMB might have accommodated around SiNPs. This excess TMB could be oxidized independent on hybridization.

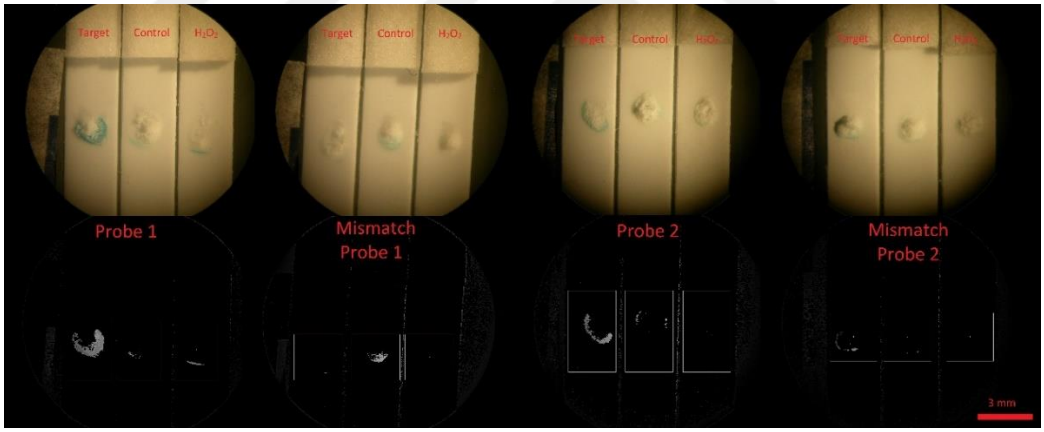

Figure 3.24: The image of LFAs including SiNPs capped with Probe-1, Mismatch Probe-1, Probe-2 and Mismatch Probe-2. ([TMB] = 5 mM, 1% H_2O_2, 0.5 mg/mL of HRP and 37°C)

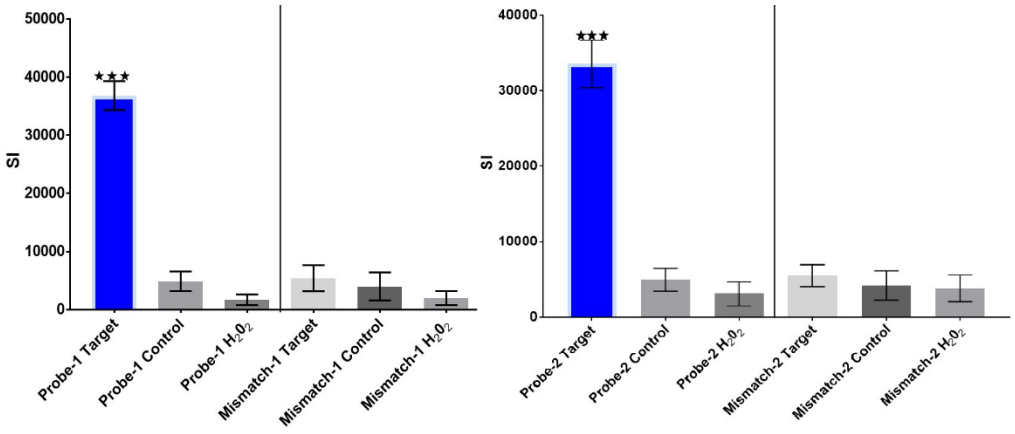

Figure 3.25: Signal Intensities of LFAs including SiNPs capped with Probe-1, Mismatch Probe-1, Probe-2 and Mismatch Probe-2. Probe-1 and Probe-2 capped SiNPs gave meaningful signals on LFAs (ANOVA, Tukey HSD test, $P<0.001$, n=6)

3.4. Sensitivity of Silica Nanoparticle Based Lateral Flow Assay

The ability of assays to detect a low concentration of a given substance was called as the sensitivity of assay. To check the sensitivity of SiNPs based LFAs, quantity of targets was gradually prepared in two ways, which are different concentrations of synthetic targets and various number of cycle in PCR.

3.4.1. Limit of Detection for Synthetic Targets

Three synthetic targets were used for Limit of detection. Target-1 and Target-2 are complementary to Probe-1 and Probe-2, respectively. Addition to complementary target, Control Target, uncomplementary to all probes, was used. Concentrations of complementary targets were started at 1000 nM. When targets with gradual concentration were applied on LFAs, Signal intensity was also measured in gradual amount. The highest amount of color was measured at 1000 nM of Target-1 and Target-2. 1000 nM of Control Target and 0 nM of Target did not form color on LFAs. The lowest concentration of synthetic targets was determined as 5 nM of synthetic targets. Synthetic targets have the same size as probes and are complementary to their own probes. Thus, hybridization made pores opened and TMB released. The perfect complementary hybridization enhanced to release TMB until 5 nM of synthetic targets. LoD for both Probe-1 and Probe-2 was determined as 5 nM of synthetic targets.

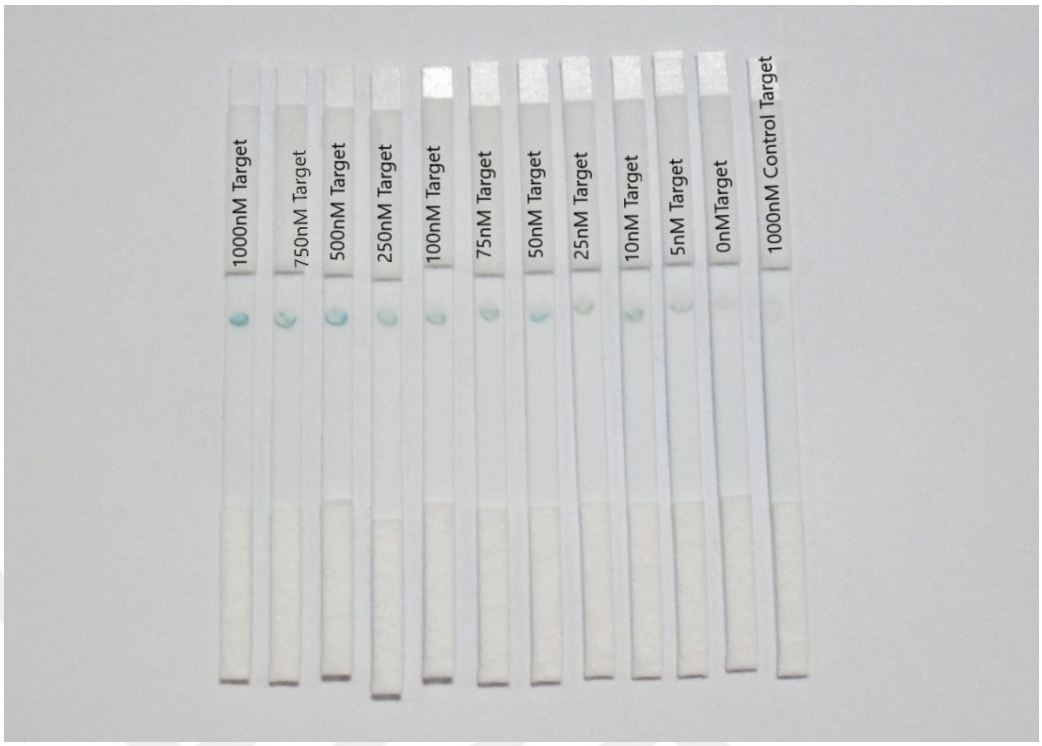

Figure 3.26: The overall images of LFAs, including Probe-1 capped SiNPs, onto which, gradual concentration of synthetic complementary Target-1 (1000 nM, 750 nM, 500 nM, 250 nM, 100 nM, 75 nM, 25 nM, 10 nM, 5 nM and 0 nM) and 1000 nM of uncomplementary Control Target were applied. ([TMB] = 5 mM, 1% H_2O_2, 0.5 mg/mL of HRP and 37ºC)

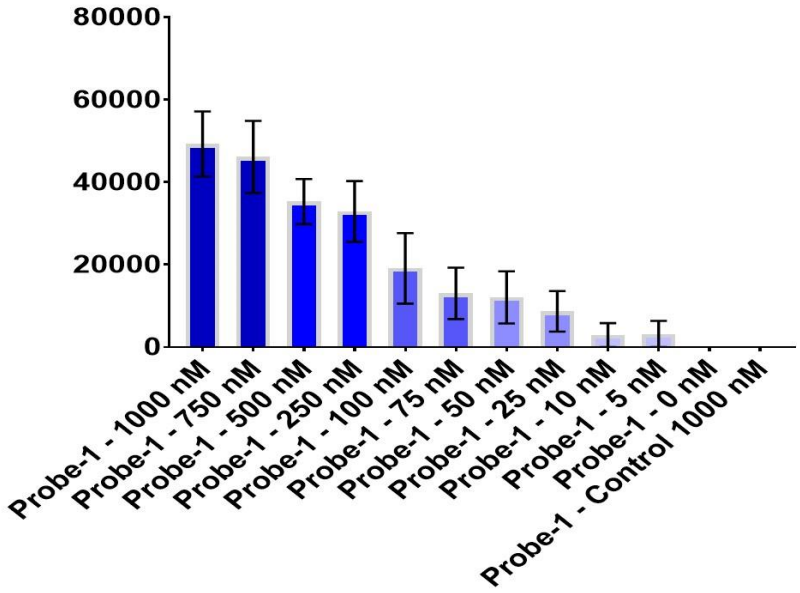

Figure 3.27: Signal Intensity of LFAs, including Probe-1 capped SiNPs, onto which gradual concentration of synthetic complementary Target-1 (1000 nM, 750 nM, 500 nM, 250 nM, 100 nM, 75 nM, 25 nM, 10 nM, 5 nM and 0 nM) and 1000 nM of uncomplementary Control Target

Figure 3.28: The overall image of LFAs, including Probe-2 capped SiNPs, onto which, gradual concentration of synthetic complementary Target-2 (1000 nM, 750 nM, 500 nM, 250 nM, 100 nM, 75 nM, 25 nM, 10 nM, 5 nM and 0 nM) and 1000 nM of uncomplementary Control Target. ([TMB] = 5 mM, 1% H_2O_2, 0.5 mg/mL of HRP and 37ºC)

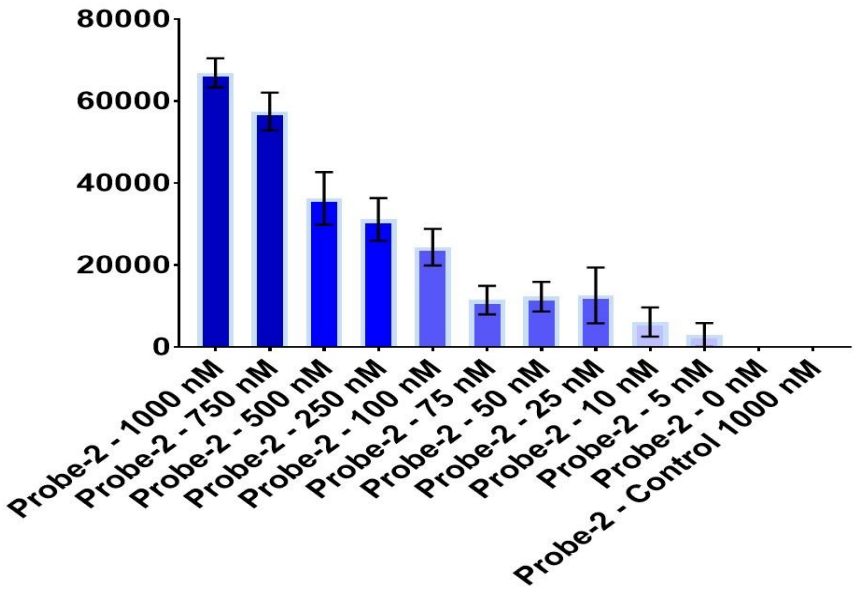

Figure 3.29: Signal Intensity of LFAs, including Probe-2 capped SiNPs, onto which, gradual concentration of synthetic complementary Target-2 (1000 nM, 750 nM, 500 nM, 250 nM, 100 nM, 75 nM, 25 nM, 10 nM, 5 nM and 0 nM) and 1000 nM of uncomplementary Control Target.

3.4.2. Limit of Detection for PCR Products

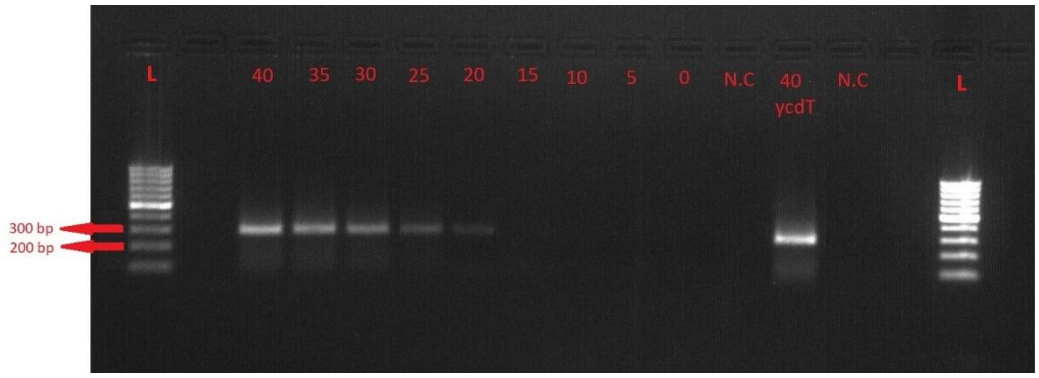

Figure 3.30: The overall image of agarose electrophoresis in which 40 cycle, 35 cycle, 30 cycle, 25 cycle, 15 cycle, 10 cycle, 5 cycle, 0 cycle and control amplicon (40 cycle) were applied.

PCR protocol in preparation of amplicon was applied by changing the number of cycle. 40 cycle, 35 cycle, 30 cycle, 25 cycle, 20 cycle, 15 cycle, 10 cycle, 5 cycle, 0 cycle of target amplicon and 40 cycle of control amplicon (*ycdT*, 292 bp) were prepared and applied onto LFAs with Probe-1 and Probe-2 Capped SiNPs. To check amplicon quantity, gel electrophoresis was run. It was observed that the amount of amplicon gradually decreased from 40 to 20 cycle. At 20 cycle, weak band was seen. When amplicons with various cycle was applied onto LFAs, until 15 cycle amplicons; signal, blue color could be generated in LFAs with complementary probes. SIs from 40 cycle to 15 cycle differentiated from 10 cycle to 0 cycle and control amplicon (ANOVA, $P<0.01$). Low amount of SIs from 10 cycle to 0 cycle and control amplicon were also recorded in assays. Some amount of TMB could be touch on SiNPs or there was leak of TMB in SiNPs. Therefore, without hybridization between probes and amplicon, a small amount of TMB might be oxidized and drove to background signals, even if washing steps existed. The reason for leakage might have been that the construction of enzyme-oxygen complex could damage ionic equilibrium on surface of SiNPs. Some of probes could run away from surface regardless of complementary amplicon.

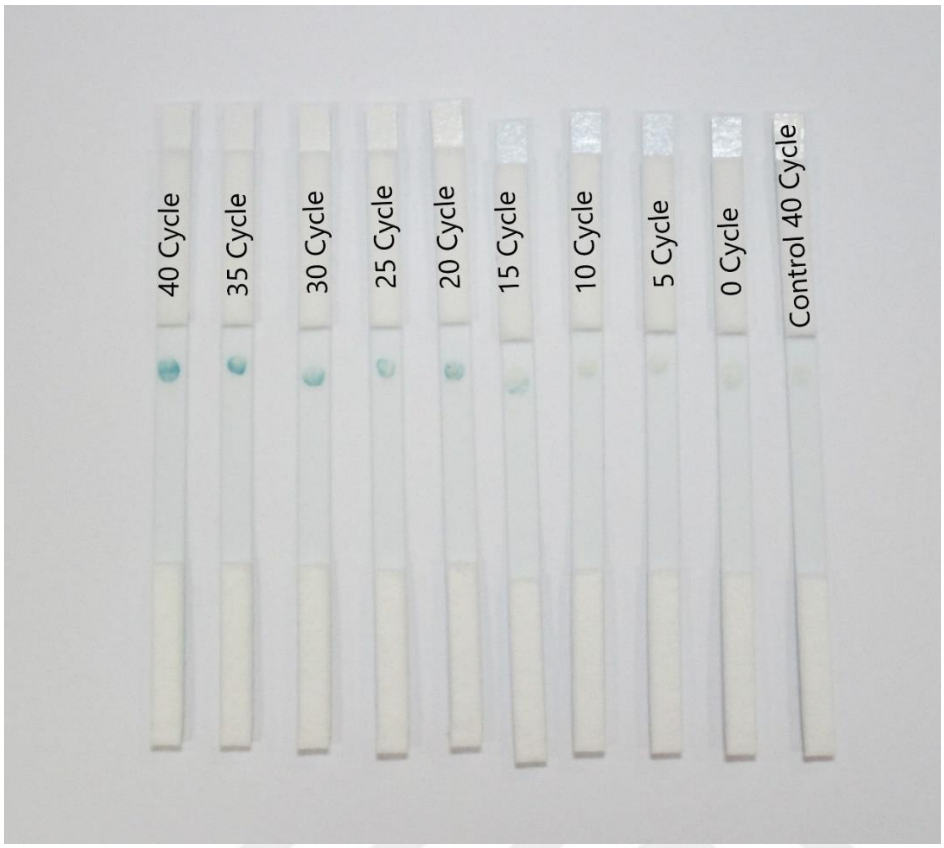

Figure 3.31: The overall image of LFAs, including Probe-1 capped SiNPs, onto which, target amplicon with various number of cycle (40, 35, 30, 25, 20, 15, 10, 5, 0) and control amplicon (40 cycle) were applied separately. Until 10 cycle, Signal could be detected on LFAs. ([TMB] = 5 mM, 1% H_2O_2, 0.5 mg/mL of HRP and 37ºC)

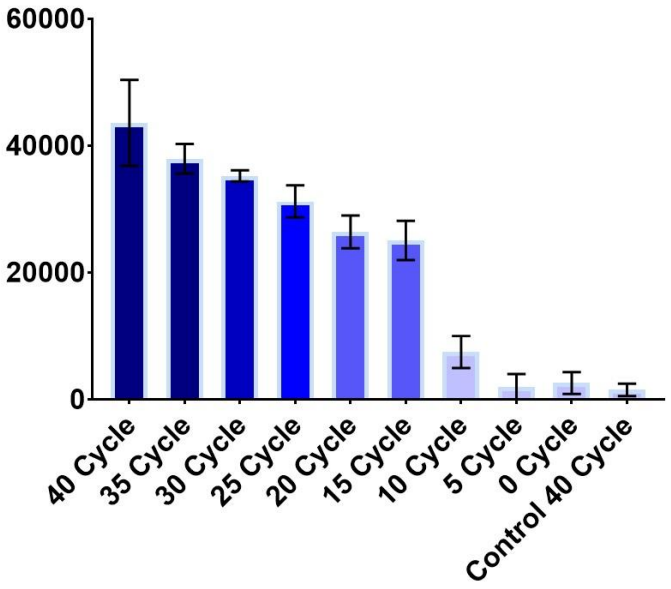

Figure 3.32: The graph of SIs on LFAs with Probe-1 capped SiNPs, onto which, target amplicon (20 ng input DNA was added in 50 µL PCR solution) with various number of cycle (40, 35, 30, 25, 20, 15, 10, 5, 0) and control amplicon (40 cycle) were applied separately. Until 10 cycle, LFAs could response complementary targets. LoD was determined as 15 Cycle.

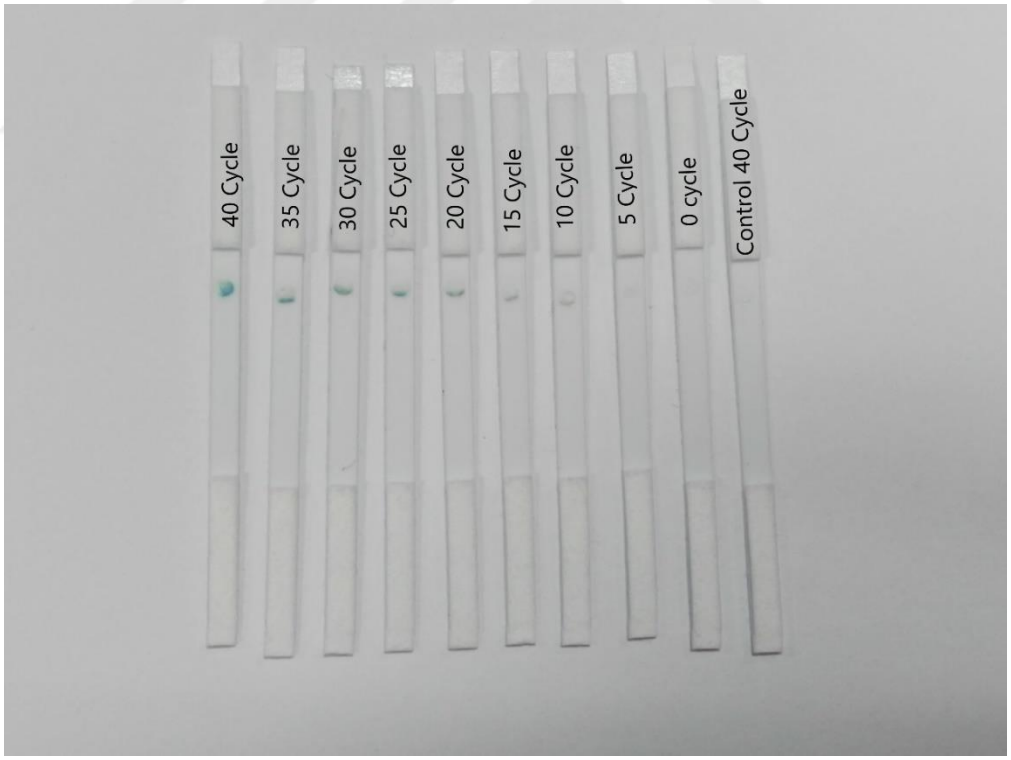

Figure 3.33: The overall image of LFAs, including Probe-2 capped SiNPs, onto which, target amplicon with various number of cycle (40, 35, 30, 25, 20, 15, 10, 5, 0) and control amplicon (40 cycle) were applied separately. Until 10 cycle, Signal could be detected on LFAs. ([TMB] = 5 mM, 1% H_2O_2, 0.5 mg/mL of HRP and 37ºC)

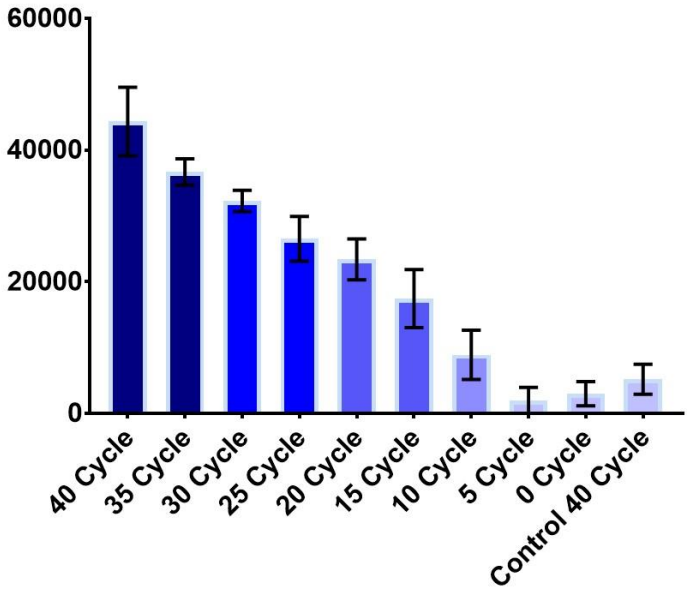

Figure 3.34: The graph of SIs on LFAs with Probe-1 capped SiNPs, onto which, target amplicon (20 ng input DNA was added in 50 µL PCR solution) with various number of cycle (40, 35, 30, 25, 20, 15, 10, 5, 0) and control amplicon (40 cycle) were applied separately. Until 10 cycle, LFAs could response complementary targets. LoD was determined as 15 Cycle.

CHAPTER 4

CONCLUSION

In this study, it was aimed to develop a novel point of care diagnostic method ensuring ASSURED criteria of WHO (Affordable, Sensitive, Specific, User-Friendly, Rapid, Equipment-free ad Deliverable to end-users). For this purpose, Silica Nanoparticles (SiNPs), which had been capped by oligonucleotide probes, were located on Lateral Flow Assay (LFA) platform. Target amplicon with complementary sequence to probes had the ability to remove probes away from SiNPs. Cargo molecule, 3,3′,5,5′-Tetramethylbenzidine (TMB) was released and oxidized by HRP-H_2O_2. The signal could be seen in blue color, which was visible with the naked eyes. However, to quantify blue color, images of LFAs were proceeded and statistically analyzed.

As a result of optimization experiments, 1% H_2O_2 was determined for proper signal propagation on LFAs even if there was non-linear correlation between signal intensity and concentration of H_2O_2. 5mM of TMB produced meaningful specific signal because of proper entrapping concentration with SiNPs, 0.5 mg/mL of HRP did not differentiate from 1 mg/mL of HRP concerning specificity and signal intensity. 0.5 mg/mL HRP was used in the colorimetric reaction system as it was more economical. To prepare adequate capped SiNPs, SiNPs were silanized at 37^{o}C for 3 hours and oligonucleotide probes capped SiNPs at 37^{o}C for an hour. Capped SiNPs were placed on LFAs platform. The organization of LFAs platform was optimized as SiNPs were located 4 mm far away from sample pad and HRP was placed 2 mm below SiNPs.

SiNPs based LFA was checked for specificity and sensitivity. In specificity experiments, as a sample, target amplicon, control amplicon and only H_2O_2 without amplicon were applied on LFAs which include complementary probes and uncomplementary probe. Target amplicon significantly differentiated from control amplicon and only H_2O_2. Additionally, Probe-1 and Probe-2 were respectively complementary to 5' end of target amplicon, and the middle of target amplicon. Any meaningful variation on response of complementary probes was not found. Therefore, the binding position could not effect on the response of SiNPs based LFAs. Sensitivity of SiNPs based LFAs was determined with synthetic targets and conventional PCR. At least 5nM of synthetic targets was determined on limit of detection (LoD) experiments of the assay. LoD of amplicon was defined with the number of cycle in PCR. 15 cycle in PCR was sufficient to observe signal on LFAs

SiNPs based LFAs specifically and sensitively recognized amplicons. The assay was rapid and accurate method. SiNPs based have potential to be one of common point of care tests for future. However, it still needs PCR equipment because amplicon was used as a sample. Thus, the assay should be improved to be user-friendly.

REFERENCES

A. Chen and S. Yang. (2015). Replacing Antibodies with Aptamers in Lateral Flow Immunoassay. *Biosensors and Bioelectronnics*, 230-242.

Akça, O. (2014). *Development f Diagnostic Platforms for Single Nucleotide Polymorphism Detection.* ANKARA: Middle East Technical University.

Alexander Libermana, Natalie Mendeza, William C. Troglerb and Andrew C. Kummelb. (2014). Synthesis and Surface Functionalization of Silica Nanoparticles for Nanomedicine. *Surf Sci Rep*.

Alfred J. Saah and Donald R. Hoover. (1997). "Sensitivity" and "Specificity" Reconsidered: The Meaning of These Terms in Analytical and Diagnostic Settings. *Lingua Medica*, 91-94.

Alizar Ulianas, Lee Yook Heng, Sharina Abu Hanifah and Tan Ling Ling. (2012). An Electrochemical DNA Microbiosensor Based on Succinimide-Modified Acrylic Microspheres. *Sensors*, 5445-5460.

Arvid, E. (2016). Salmonellosis. In E. T. Bope, *Conn's Current Threapy 2016* (pp. 188-192). Philadelphia: Elsevire.

B. Ngom, Y. Guo,Wang X, Bi D. (2010). Development and Applciation of Lateral Flow Test Strip Technology for Detection of Infectious Agents and Chemcal Contaminats. *Analytical and Bioanalytical Chemistry*, 1113-1135.

Bhalla, N. (2016). Introduction to biosensors. *Essays in Biotechnoogy*, 1-8.

Brands, D. (2006). Salmonella Strikes at the Senior Prom. In *Deadly Disease and Epidemics Salmonella* (p. 13). Chelsea House Publishers.

Brenner. (2000). Salmonella Nomenclature. *Journal of Clinical Microbiology*, 2465–2467.

Caroline A Schneider, Wayne S Rasband and Kevin W Eliceiri. (2012). NIH Image to ImageJ: 25 Years of Image Analysis. *Nature Methods* , 671–675 .

Chiu, C. H. (2010). Salmonella, Non-Typhoidal Species (S. Choleraesuis, S. Enteritidis, S. Hadar, S. Typhimurium). *Infectious Disease and Antimicrobial Agents*.

Claudie Parolo and Arben Merkoçi. (2013). Paper Basen Nanobiosensors for Diagnostics. *Chem. Soc. Rev*, 450-457.

Claudio Parolo, Arben Merkoçi. (2013). Paper Based Nanobiosensors for Diagnostics. *Chem. Soc. Rev.*, 450-457.

Cooke, F. J. (2007). Current Trend in the Spread and Occurence of Human Salmonellosis: MolecularTyping and Emerging Antibiotic Resistance. In D. M. Mikael Rhen, *Salmonella Molecullar Biology and Pathogenesis.* Norfolk, UK: Horizon Bioscience.

Cristina Giménez et al. (2015). Gated Mesoporous Silica Nanoparticles for the Controlled Delivery of Drugs in Cancer Cells. *Langmuir*, 3753-3762.

D. Rath, S. Rana and K. M. Parida. (2014). Organic Amine-Functionalized Silica Based Mesoporous MaterialsÇ an Update of syntheses and Catalytic Applications. *The Royal Society of Chemistry*, 57111-57124.

Dan Mo and Liang Hu. (2017). Cadmium-Containing Quantum Dots: Properties, Applications and Toxicity. *Appl Microbiol biotechnology*, 2713-2733.

Daniel Quesada Gonzalez, Arben Merkoçi. (2015). Nanoparticles-Based Lateral Flow Biosensors. *Biosensors and Bioelectronics*, 47-63.

Danielsson, B. (1991). Calorimetric Biosensors. *Biochemical Society Transaction*, 26-28.

Department of Economic and Social Affairs. (2004). *World Population to 2300.* New York: United Nations,.

Dougnon, H. B.-M. (2016). Review on the Problematic of Salmonellosis and Interests of Traditional Herbs in the Treatment. *Clinical Microbiology*.

E. B. Bahadır and M. K. Sezgintürk. (2016). Lateral Flow Assays: Principles, Design and Labels. *Trends in Analytic Chemistry*, 286-306.

E. Climent et al. (2010). Controlled Drug Delivery Using Oligonucleitide-Capped Mesoporous Silica Nanoparticles. *Angewandthe Chemie*, 7281-7283.

EFSA and ECDC. (2016). *The European Union Summary Report on Trends and Sources of Zoonoses,*. Parma: EFSA Journal.

Elaine Scallan et al. (2011). Foodborne Illness Acquired in the United States—Major Pathogens. *Emerging Enfectious Diseases*.

Elaine Scallan, Patricia M. Griffin, Frederick J. Angulo, Robert V. Tauxe, Robert M. Hoekstra. (2011). Foodborne Illness Acquired in the United States—Unspecified Agents. *Emerging Enfectious Diseases*.

Eleanor G. Rogan, Patricia A. Katomski, Robert W. Roth, and Ercole L. Cavalieri. (1979). Horseradish Peroxidase/Hydrogen Peroxide-catalyzed Binding of Aromatic Hydrocarbons to DNA. *The Journal of Biological Chemistry* , 7055-7059.

FDA. (2016). *Foodborne Illnesses: What You Need to Know*. Washington: U.S. Department of Health and Human Services.

Gao L, Wu J and Gao D. (2011). Enzyme-Controlled Self-Assembly and Transformation of Nanostructures in a Tetramethylbenzidine/Horseradish Peroxidase/H2O2 System. *ACS nano*, 6736-6742.

Gerard, M. (2002). Application of Conducting Polymers to Biosensors. *Biosensors&Bioelectronics*, 346-359.

H. V. Hsieh, J. L. Dantzler and B. H. Weigl. (2017). Analytical Tools to Improve Optimization Procedures for Laeral Flow Assays. *Diagnostics*.

Hassani, S. (2017). Biosensors ad Their Applications in Detection of Organophosphorous Pesticides in the Environment. *Arch. Toxicol.*, 109-130.

J. Singh, S. Sharma, S. Nara. (2015). Evaluation of gold nanoparticle based lateral flow assays for diagnosis of enterobacteriaceae members in food and water. *Food Chemistry*, 470-483.

J.E. Galan, C. Ginocchio, P. Costeas, . (1992). Molecular and functional characterization of the Salmonella invasion gene invA: homology of InvA to members of a new protein family. *Journal of Bacteriology*, 4338-4349.

Jason R. Andrews, Edward T. Ryan. (2015). Diagnostics for Invasive Salmonella Infections: Current Challenge and Future Directions. *Vaccine*.

Jie Yan and John F. Marko. (2004). Localized Single-Stranded Bubble Mechanism for Cyclization of Short Double Helix DNA. *PHYSICAL REVIEW LETTERS*.

John A. Crump, Maria Sjölund-Karlsson, Melita A. Gordon, Christopher M. Parrye. (2015). Epidemiology, Clinical Presentatio, Laboratory Diagnosis, Antimicrobial Resistance and Antimicrobial Management of Invasive Salmonela Infections. *Clinical Microbiology Reviews*, 901-937.

John A. Howarter and Jeffrey P. Youngblood. (2006). Optimization of Silica Silanization by 3-Aminopropyltriethoxysilane. *Langmuir*, 11142-11147.

Josefa Hernander- Ruiz, Marino B. Arnao, Alexander N. P. Hiner, Francisco Garci. (2001). Catalase-like activity of horseradish peroxidase: relationship to enzyme inactivation by H2O2. *Biochem.*, 107-114.

K. M. Koczula and A. Gallotta. (2016). Lateral FLow Assays. *Essays in Biochemistry*, 111-120.

Kavita Arora, Subhash Chand. D. Malhotra . (2006). Recent developments in bio-molecular electronics techniques for food pathogens. *Analytica Chimica Acta*, 259–274.

Khosla, S. (1993). Gastric Juice Secretion in typhoid fewer. *Postgrad Med. J.*, 121-123.

Kwon, S. (2013). Silica-Based Mesoporous Nanoparticles for Controlled Drug Delivery. *Journal of Tissue Engineering*.

L. Gao, J. Zhuang, L. Nie and J. Zhang. (2007). Intirinc Peroxidase Like Activity of Ferromagnetic Nanoparticles. *Nature Nanotechnology*, 577-583.

Linda Dekker, Karen M Polizzi. (2017). Sense and sensitivity in bioprocessing — detecting cellular metabolites with biosensors. *Current Opinion in Chemical Biology*, 31-36.

Linda Dekker; Karen M Polizzi. (2017). Sense and Sensitivity in Bioprocessing - detecting CUlular Metabolites with Biosensors. *Current Opinion oin Chemical Biology*, 31-36.

Luis Pascual et al. (2014). Oligonucleotide-capped mesoporous silica nanoparticles as DNA-responsive dye delivery. *The Royal Society of Chemistry*.

M. J. Raeisossadati, N. M. Danesh and F. Borna. (2016). Lateral Flow Based Immunobiosensors for detection of food contaminants. *Biosensors and Bioelectronics*, 235-246.

Mar Oroval et al. (2013). An aptamer-gated silica mesoporous material for thrombin detection. *Chem. Com.*

Mathieu Etienne, Alain Walcarius. (2003). Analytical investigation of the Chemical Reactivity and Stability of Aminopropyl-Grafted Silica in Aqueous Medium. *Talanta*, 1173-188.

Mello, L. D. (2002). Review of the Use of Biosensors as Analytical Tools in the Food and Drink Industries. *Food Chemistry*, 237-256.

Michael Holzinger, Alen Le Goff and Serge Cosnier. (2014). Nanomaterials for Biosensing Applicaitions: a Review. *Frontiers in Chemistry*.

Nebraska Redox Biology Center Educational Portal. (2017, june 29). Retrieved from Hydrogen Peroxide: http://genomics.unl.edu/RBC_EDU/hp.html

Nur Mustafaoglu, Tanyel Kiziltepe, Basar Bilgicer. (2017). Site-Specific Conjugation of an Antibody on a Gold Nanoparticle Surface for One-Step Diagnosis of Prostate Specific Antigen with Dynamic Light Scattering. *Nanoscale*.

Ohad Gal-Mor, Erin C. Boyle, and Guntram A. Grassl. (2014). Same Species, Different Diseases: How and Why Typhoidal an Non-Typhoidal Salmonella Enterica Serovars Differ. *Frontiers in Microbiology*.

P. D. Josephy, T. Eling and R. P. Mason. (1982). The Horseradish Peroxidase-catalyzed Oxidationof 3,5,3',5'-Tetramethylbenzidine. *The Journel of Biological Chemistry*, 3669 -3675.

Porwollik, S. (2004). Characterization of Salmonella enterica Subspecies I Genovars by Use of Microarrays. *Journal of Bacteriology* , 5883-5898.

Pui, C. F. (2011). Salmonella: A foodborne pathogen. *International Food Research Journal* , 465-473.

Qingkun Kong, Tanhu Wang, Lina Zhang, Shenguang Ge, Jinghua Yu. (2016). A Novel Microfluidic Paper Based Colorimetric Sensor Based on Molecularly İmprinted Polymer Membranes for Highly Selective and Sensitive detection of Bisphenol A. *Sensors and Actutors B: Chemical*, 130-136.

R. Kumar, C. K. Singh, S. Kamle, R.P. Sinha. (2010). Development of Nanocolloidal GOld Based immunochromatographic Assay for Rapid Detection of Transgenic Insectisidal Protein in Genetically Modified Crops. *Food Chemistry*, 1298-1303.

R. M. Fartila, S. G. Mitchell, P. D. Pino, V. Grazu and J. M. Fuente. (2014). Strategies for the Biofunctionalization of Gold and Iron Oxide Nanoparticles. *Langmuir*, 15057-15071.

R. M. Kong, X. B. Zhang, Z. Chen and W. Tan. (2011). Aptamer Assembled Nanomaterials for Bİosesing and Biomedical Applciations. *small*, 2428-2436.

Rafael A. Bini, at al. (2011). Synthesis and functionalization of magnetite nanoparticles with different amino-functional alkoxysilanes. *Journal of Magnetism and Magnetic Materials*, 534–539.

Rahn K, De Grandis SA, Clarke RC, McEwen SA, Galán JE, Ginocchio C, Curtiss R, Gyles CL. (1992). Amplification of an invA gene sequence of Salmonella typhimurium by polymerase chain reaction as a specific method of detection of Salmonella. *Molecular and Cellular Probes* , 271-279.

Robert G. Acres et al. (2014). Molecular Structure of 3-Aminopropyltriethoxysilane Layers Formed on Silanol-Terminated Silicon Surfaces. *The Journal of Physical Chemistry C*, 6284-6297.

S. H. Wu, C. Y. Mou and H. P. Lin. (2013). Synthesis of Mesoporous Silica Nanoparticles. *Chem. SOc. Rev.*, 3862-3875.

Scheller, F. W. (2001). Research and Development in Biosensors. *Current Opinion in Biotechnology*, 35-40.

Seung Min Yoo, Sang Yup Lee. (2016). Optical Biosensors for the Detection of Pathogenic Microorganisms. *Trends ib Biotechnology*, 7-25.

Sigma-Aldrich. (2017, July 4). *3,3',5,5'-Tetramethylbenzidine.* Retrieved from Sigma Aldich: http://www.sigmaaldrich.com/catalog/product/aldrich/860336?lang=en&region=TR

Sigma-Aldrich. (2017, July 4). *Peroxidase Enzymes.* Retrieved from Sigma Aldrich: http://www.sigmaaldrich.com/life-science/metabolomics/enzyme-explorer/analytical-enzymes/peroxidase-enzymes.html

Sun-Mi Lee et al. (2016). Real-time monitoring of 3D cell culture using a 3D capacitance biosensor. *Biosensors and Bioelectronics*, 56-61.

T Gregory Drummond, Michael G Hill, Jacqueline K Barton. (2003). Electro Chemical DNA Sensors. *Nature Biitechnology*, 1192-1198.

Tamaki Soga, Yusuke Jimbo, Koji Suzuki and Daniel Citterio. (2013). Inkjet-Printed Paper Based Colormetric Sensor Array for the Discrimination of Volatile Primary Amines. *Analytical Chemistry*, 8973-8978.

Tatiana Andreani, Amelia M. Silva, Eliana B. Souto. (2015). Silica-Based Matrices: State of the Art and New Perspectives for therapeutic Drug Delivery. *Biotechnology and Applied Biochemistry*, 754-764.

Thevenot, D. R. (2001). Electrochemical Biosensors: Recommended Definitions and Classification. *biosensors & Bioelectronics*, 121-131.

Uzzau, S. (2000). Host adapted serotyps of Salmonella enterica. *Epidemiol. Infect.*, 229-255.

V. C. Ozalp and T. Schafer. (2011). Aptamer-Based Switchable Nanovalves for Stimuli responsive Drug Delivery. *Chemistry-A European Journal*, 9893-9895.

Verma N, Sharma R. (2017). Bioremediation of Toxic Heavy Metals: A Patent Review. *Recent Patents in Bitechnology*.

Verma, M. L. (2017). Nanobiotechnology advances in enzymatic biosensors for the agri-food industry. *Environmental Chemşstry Letters*, 1-6.

Vigneshvar, S. (2016). Recent Advances in Biosensor Technology for Potential Aplications. *Frontiers in Bioengineering and Biotechnology*.

W. Zhang, X. X. Hu, X. B. Zhang. (2016). Dye-Doper Fluoresecent Silica Nanoparticles for Live Cell and In Vivo Bioimaging. *Nanomateriials*.

Wenzhang Cha et al. (2017). Mesoporous Silica Nanoparticles as Carriers for INtra cellular Delivery of Nucleic Acids and SubsequentTherapeutic Applications. *Molecules*.

WHO. (2013). *Salmonella (non-typhoidal).* Geneva: World Health Organization.

WHO. (2015). *WHO Estimates of The Global Burden of Foodborne Diseases.* Geneva: WHO.

Witucki, G. L. (1992). A Silane Primer: Chemistry and Applciatons of Alkoxyl Silanes. *A journal of Coating Technology*.

X. Wang, R. Niessner, D. Tang and D. Knopp. (2016). Nanoparticle-based immunosensors and immunoassays for aflatoxins. *Analytica Chimica Acta*, 10-23.

Yujun Song, Konggang Qu, Chao Zhao, Jinsong Ren, and Xiaogang Qu. (2010). Graphene Oxide: Intrinsic Peroxidase Catalytic Activity and Its Application to Glucose Detection. *Advaced Materials*, 2206–2210.

Zhan-Hui Wang, Gang Jin. (2003). Silicon surface modification with a mixed silanes layer to immobilize proteins for biosensor with imaging ellipsometry. *Colloids and Surface B.*

Zonci Li, Jonathan C. Barnes, Aleksandr Bosoy, J. Fraser Stoddart, Jeffrey I. Zink. (2012). Mesoporous silica Nanoparticles in Medical Applications. *Chem. SOc. Rev.*, 2590-2605.

APPENDIX A

BUFFERS AND SOLUTIONS

Tryptic Soy Broth (TSB)

17 g of casein, 3 g of soya peptone, 5 g of NaCl and 2.5 g of K_2HPO_4 were weighed and completely dissolved in 1L of distilled H_2O. pH of solution was set to 7.3 with 1M of NaOH and 1M of HCl. Suspension was sterilized with autoclave at 121^oC for 15 minutes. The broth was stored at 4 ^oC. it was taken 30 minutes from fridge before usage of TSB.

Tryptic Soy Agar (TSA)

17 g of casein, 3 g of soya peptone, 5 g of NaCl, 2.5 g of K_2HPO_4 and 15 g of agar were weighed and completely dissolved in 1 L of distilled H_2O. pH of solution was set to 7.3 with 1M of NaOH and 1M of HCl. Suspension was sterilized with autoclave at 121^oC for 15 minutes. After autoclaving done and temperature was around 80 ^oC, it was distributed into sterile plates under laminar hood. To check sterility, at least one of plate was carried on 37^oC and waited at room temperature. TSA was freshly used.

Luria-Bertani Broth (LBB)

10 g of tryptone, 5 g of yeast extract and 10 g of NaCl were weighed and dissolved in 1L of distilled H_2O. pH was adjusted to 7.0 with 1M of NaOH and 1M of HCl.

The medium was sterilized with autoclave for 150 minutes at 121°C. The broth was stored at 4 °C. it was taken 30 minutes from fridge before usage of LBB.

Luria-Bertani Agar (LBA)

10 g of tryptone, 5 g of yeast extract 10 g of NaCl and 10 g of agar were weighed and dissolved in 1L of distilled H_2O. pH was adjusted to 7.0 with 1M of NaOH and 1M of HCl. Solution was autoclaved for 150 minutes at 121°C. After autoclaving done and temperature was around 80 °C, it was filled into sterile plates under laminar hood. To check sterility, at least one of plate was carried on 37°C and waited at room temperature. LBA was freshly used.

Dulbecco's Phosphate Buffered Saline (Ca^{++} Mg^{++} Free PBS)

0.2 g of potassium chloride(KCl), 0.2 g of monobasic potassium phosphate (KH_2PO_4), 8 g of sodium chloride (NaCl), and 1.74 g of dibasic sodium phosphate (Na_2HPO_4.7H20) were dissolved in 0.9 liter of distilled water. pH of solution was adjusted to 7.4 with 1M of NaOH and HCl. The volume was completed to 1 liter with water. PBS was sterilized with 0.22 μm filter and stored at 4 °C.

TMB Stock Solution

0.240 g of 3,3′,5,5′-Tetramethylbenzidine (TMB) was weighed and dissolved in 1 mL of dimethyl sulfoxide (DMSO).

TMB Working Solutions

100 μL of TMB stock solution and 400 μL of DMSO were mixed and 0.2M of TMB solution was prepared. 250 μL of TMB stock solution and 250 μL of DMSO were mixed and 0.5M of TMB solution was prepared.

HRP solutions

0.25 mg of HRP was weighed and dissolved in 250 μL of filtered MilliQ for 1mg/mL. 0.1 mg of HRP was weighed and dissolved in 200 μL of filtered for 0.5 mg/mL

H_2O_2 solution

10 mL of MilliQ was filled into a centrifuge tube. 286 μL of MilliQ was discarded from the centrifuge tube and 286 μL of 35% H_2O_2 solution was added. By this way, 1%(w/v) (0.294 M), 1.5% (0.441 M), 2.5% (0.735 M) and 3.5% (1.03 M) of H_2O_2 solutions were prepared to freshly use in LFAs.

APPENDIX B

SEQUENCES OF PRIMERS, PROBES, TARGETS

Table A.A: Sequences of primers with sequences, Tm and GC%

Primers	Sequence (5 → 3)	Tm	GC%
InvA Forward Primer	GTG AAA TTA TCG CCA CGT TCG GGC AA	66.45	50.00
InvA Reverse Primer	TCA TCG CAC CGT CAA AGG AAC C	63.37	54.55
ycdT Forward Primer	AGC ATA CGA CCA GAT GAC CTT T	59.50	45.45
ycdT Reverse Primer	CAT CCC TCA CAA CCA CCT TAT TAC	59.12	45.83

Table A.B: Sequences of Probes

Probes	Sequence (5 → 3)
Probe-1	CCA ATA ACG AAT TGC CCG AAC GTG GCG ATA ATT T
Probe-2	TAA CGA TAA ACT GGA CCA CGG TGA CAA TAG AGA A
Uncomplementary Probe	TAT GGT GTA GGT CGA GGC AGG TGT TTG CAG TCA G

Table A.C: Sequences of synthetic targets

Synthetic Targets	Sequence (5 → 3)
Synthetic Target-1	AAA TTA TCG CCA CGT TCG GGC AAT TCG TTA TTG G
Synthetic Target-2	TTC TCT ATT GTC ACC GTG GTC CAG TTT ATC GTT A
Control Target	GGT CAG GTC TGG GTA AAA ATG TCA AGC GGT AGG T